Volume-based phase stability analysis including capillary pressure

Dan Vladimir Nichita

Version of Record: https://www.sciencedirect.com/science/article/pii/S0378381219301384
Manuscript_587f08b216429ada832a031313425949

Volume-based phase stability analysis including capillary pressure

Dan Vladimir Nichita [1,*]

[1] *CNRS UMR 5150, Laboratoire des Fluides Complexes et leurs Réservoirs, Université de Pau et des Pays de l'Adour, B.P. 1155, 64013 Pau Cedex, France*

Abstract

The effect of capillary pressure on phase equilibrium is very important in tight formations, such as shale oil and gas reservoirs. In confined fluids, the capillary pressure induced by highly curved interfaces causes bubble points suppression and an inflated dew point locus, with a shift of cricondentherm points towards higher temperatures, as compared to the bulk fluid. In the conventional phase stability testing including capillary pressure, the problem is solved using the classical tangent plane distance (TPD) function (related to the Gibbs free energy surface) and mole numbers as primary variables. In this work, a volume-based approach (in which the equation of state needs not to be solved for volume) is used to solve this problem, as a bound and linear inequality constrained minimization of a TPD function with respect to the component molar densities. A modified Cholesky factorization (to ensure a descent direction) and a two-stage line search procedure (to ensure that iterates remain in the feasible domain and the objective function is decreased) are used in Newton iterations; a proper change of variables strengthens the robustness. The Weinaug-Katz equation (widely used in chemical and petroleum industry), which is a function of molar densities only, is used for interfacial tensions; the additional partial derivatives in the gradient vector and Hessian matrix have very simple expressions, unlike in conventional formulations. The proposed method is tested for two hydrocarbon mixtures (an oil and a gas condensate) in a wide range of pressures, temperatures and curvature radii, with a special attention paid to the convergence behavior near the singularities, that is, the stability test limit locus (STLL) and the spinodal. The method proves to be highly robust and exhibits fast convergence, showing a similar convergence behavior and almost the same computational effort as in the case of a bulk fluid. The results are only slightly different from conventional methods (except at high curvatures near the cricondentherm and at low pressures); differences are due to the fact that the dependence of capillary pressure on composition is taken into account in deriving the stationarity conditions, unlike in the conventional approach. The proposed

method is not dependent on the thermodynamic model and can be used with any capillary pressure representation in which the interfacial tension model is explicit in molar densities.

Keywords: phase stability, capillary pressure, tangent plane distance, volume-based, Newton method, modified Cholesky factorization, convergence

---

* Address correspondence to Dan Vladimir Nichita, E-mail: dnichita@univ-pau.fr

1. Introduction

The thermodynamic behavior of mixtures in porous media differs from that of a bulk fluid (i.e., at infinite curvature radius) due among other factors to the action of the capillary forces. Early experimental work of Sigmund et al. [1] showed that the effect of curved interfaces on hydrocarbon phase behavior is not significant except for very small curvature radii. Similar conclusions were drawn by Danesh et al. [2] by visual examination of retrograde condensation in porous media. Tindy and Raynal [3] reported relative differences of a few percent between the saturation pressures observed in PVT cells and porous media. A detailed description of phase equilibrium and stability under the influence of capillary forces was given by Shapiro and Stenby [4,5]. Brusilovski [6] performed saturation pressure and vapor-liquid equilibrium calculations (using an equation of state and Newton iterations to solve the nonlinear systems of equations) including the capillary pressure induced by curved interfaces and reported an increase in retrograde dew point pressures (measured in the gas phase, considered as the non-wetting phase) and a decrease in bubble point pressures (measured in the liquid phase), as compared with bulk saturation pressures. In fact, it was shown later that the picture is more complex, with a shift of cricondentherm points towards higher temperatures and an inflated dew point locus [5-10].

Phase equilibrium including capillarity effects is becoming a hot topic and many papers have been published in the last few years [7-26] (this reference list is far from being exhaustive), most of them related to the increasing interest of the petroleum and gas industry in tight formations and shale oil and gas reservoirs, in which nano-scale pores may be dominant.

At very small capillary radii, the impact of capillarity on phase equilibrium is questionable and the effects of geometrical confinement [27,28] and adsorption [19,29] are predominant and must

be considered. Santiso and Firoozabadi [30] stated that the parachor model for interfacial tensions is valid only for capillary radii greater than 5 nm. Jin and Firoozabadi [19] considered that interface curvature affects phase behavior for pores larger than 10 nm. This limit is taken as 5-10 nm by Nojabaei et al. [13]. In this paper, only the influence of capillary pressure is considered (confinement and adsorption effects are not addressed) and calculations are performed for $r \geq 5\,\text{nm}$. It must be noted that this lower limit need to be taken cautiously; on the other hand, this paper is intended to provide an advanced numerical method (with a detailed analysis of convergence behavior, usually not given in papers dedicated to this subject), rather than focusing on the physical model.

Whatever the type of phase equilibrium calculations (phase stability, phase splitting or saturation points calculations), in the conventional approach (in the frame of PT-based thermodynamics, with the Gibbs free energy as the core function), the equilibrium equations are solved together with the capillary pressure (Young-Laplace) equation [31], with the interfacial tension as a function of pressure and composition at a given temperature.

Various two-phase [5,6,11,16,19,20-22] and three-phase [17,24] flash calculation methods considering capillary pressure, as well as their implementations in compositional reservoir simulators [13,20,21,25] were proposed in the last few years. Direct calculations of phase boundaries with capillarity were performed by Brusilovski [6], Nojabaei et al. [13], Pang et al. [14], Li et al. [15]. Sandoval et al. [7] (with some interesting insights on the multicomponent Clapeyron equation), and Zuo et al. [23] automatically constructed the phase envelopes in the presence of capillary effects.

Conventional phase stability testing including capillary effects has also been recently addressed [9,20,24,25]. In a detailed study on phase stability, Sherafati and Jessen [9] used successive substitution (SSI) and Newton iterations to solve the nonlinear system of equations. Kou and Sun [26] derived a TPD function and proposed an evolutionary dynamic method based on the convex-concave splitting of the Helmholtz free energy density, applied to pure components and binary mixtures.

Phase stability testing is one of the most important type of thermodynamic calculations [32,33]. It assesses the state of a fluid mixture (stable in the single phase state, or splitting in two or more equilibrium phases) and it is commonly used in phase boundary calculations, initialization of phase split calculations and validation of flash calculation results. An algorithm for phase stability testing must be both robust and fast; this is particularly important in compositional reservoir simulation, where it is common to perform phase stability tests a huge number of times during a simulation run and failures are not allowed (or in any other kind of simulator which repeatedly calls a phase stability routine a large number of times).

An alternative to conventional phase equilibrium calculations is given by the so-called volume-based approach [34], in which the volume is treated as a primary variable and thus there is no need to solve the EoS for volume (this feature may be particularly attractive for highly complex EoS). The solution of the phase equilibrium problem is sought (at temperature and moles specifications) in the composition-volume space (the Helmholtz free energy is the central thermodynamic potential, for which mole numbers, volume and temperature are the natural variables) or in the component molar densities space (in the so-called isochoric thermodynamics [35], in which the Helmholtz energy density is the central thermodynamic potential), rather than in the compositional space. In volume-based methods, simpler partial derivatives (no implicit functions are involved) are required for assembling th Hessian or Jacobian matrices. Volume-based phase stability testing methods were presented for bulk fluids by Nagarajan et al. [36], Nichita et al. [37], Nichita [38] (at pressure and temperature specifications) and by Nichita et al. [39], Mikyška and Firoozabadi [40], Castier [41] and Nichita [42].

Volume-based methods for phase equilibrium calculations seem to be particularly suited if capillary pressure is taken into account. Most interfacial tension models are explicit in volume and mole numbers or in component molar densities, which are precisely the primary variables in volume-based methods. Moreover, the partial derivatives of interfacial tension are much simpler than those in the conventional methods.

This paper addresses numerical issues related to phase stability testing including capillary pressure in the frame of isochoric thermodynamics. A volume-based approach is proposed, based on the phase stability criterion recently derived by Kou and Sun [26] (with component molar densities as primary variables). It is shown that the gradient vectors and Hessian matrices for the bulk case and for the case with capillary effects differ by terms having very simple expressions, depending only on component molar densities. A Newton method with modified Cholesky factorization and a two-stage line search procedure is used in the minimization of the TPD function. Robustness and speed observed in the bulk case seems not to be influenced by the inclusion of capillarity. The Weinaug-Katz [43] equation (widely used in chemical and petroleum industry), in which the interfacial tension is a function of molar densities only, is used in this work.

The paper is structured as follows. First, conventional stability testing with capillary pressure and bulk volume-based stability testing are presented, then the proposed volume-based stability testing with capillary pressure is introduced. Results of numerical experiments on representative hydrocarbon mixtures are presented and commented before concluding.

2. Conventional phase stability testing with capillary pressure

This section briefly presents the capillary pressure equation and some considerations on the conventional approach in phase stability testing with capillary pressure difference at pressure and temperature specifications (PT stability).

According to the Young-Laplace equation [31], for a cylindrical pore, the capillary pressure P_C is

$$P_C = P_V - P_L = \frac{2\sigma\cos\theta}{r} \tag{1}$$

where r is the radius of curvature and θ is the contact angle of the meniscus with the pore wall. Often, $\theta = 0$ (complete wetting of the liquid phase) is considered.

For pure components, the interfacial tension is given by the Macleod [44] and Sugden [45] relation

$$\sigma^{1/E} = \Pi(\rho_L - \rho_V) \tag{2}$$

where Π is the parachor, E is a scaling factor and ρ is the molar density.

For mixtures, the interfacial tension is given by Weinaug and Katz [43]

$$\sigma^{1/E} = \sum_{i=1}^{nc} \Pi_i (x_i\rho_L - y_i\rho_V) \tag{3}$$

with the scaling factor $E = 4$ (various other values were proposed for E, ranging from 3.66 ton 3.91 [9]).

Recently, several papers [9,20,24,25] addressed the conventional phase stability testing with capillary pressure, in which the equilibrium equations (equality of chemical potentials of the feed and the trial phase) are solved together with the capillary pressure equation. A detailed analysis is given by Sherafati and Jessen [9], who used Michelsen's [32] stability criterion based on a modified TPD function and presented two formulations of the Newton method (with different implicitness levels, depending on whether the pressure of the trial phase, P_w, is an independent variable or it is explicitly updated). An SSI method is also proposed in Ref. [9], with a lagged update of P_w, in which an SSI iteration is carried out exactly as for the bulk fluid to update mole numbers in the trial phase, then P_w is updated explicitly from the capillary pressure equation. This latter method is used in this work to obtain a basis of comparison for the proposed volume-based method.

However, by solving together the equilibrium equations together with the capillary pressure equation, the computational problem is no longer a minimization problem (as in the bulk case), but an equation-solving problem, with a non-symmetric Jacobian matrix, thus one cannot take advantage of symmetry, neither in building the matrix, nor in the resolution of the linear system. Moreover, the TPD function cannot be tracked and the convergence behavior is expected to be more sensitive to the quality of the initial guess. Convergence speed is inherently decreased when lagged updates are used for the pressure in the trial phase.

In the Newton method, some partial derivatives (of chemical potential with respect to pressure and of capillary pressure with respect to pressure and to mole numbers) are additionally required as compared to the bulk phase stability testing; implicit functions are involved in the differentiation process to obtain these derivatives.

3. Volume-based phase stability testing

The first volume-based phase stability criterion was suggested by Michelsen [32] (in mole fractions and molar volume). Nagarajan et al. [36] first proposed a TPD function of component molar densities and temperature, derived from the Helmholtz free energy density difference between an infinitesimal two-phase and a single phase mixture and performed stability tests at pressure and temperature specifications. At temperature, volume and moles specifications, derivations of the stability criterion (which is formally the same as in the PT case) can be found in Mikyška and Firoozabadi [40] and Castier [41], starting from the Helmholtz free energy as a function of temperature, volume and mole numbers. Several calculation methods for volume-based phase stability testing were presented [36-42].

In terms of component molar densities, the reduced TPD function is (at constant temperature, $T = T_{spec}$) [36]

$$D(\mathbf{d}) = \sum_{i=1}^{nc} d_i \left[\ln f_i(\mathbf{d}) - \ln f_{iz}(\mathbf{d}_\mathbf{z})\right] - \frac{P(\mathbf{d}) - P_z(\mathbf{d}_\mathbf{z})}{RT} \tag{4}$$

where the index z refers to the feed (reference phase) of composition $\mathbf{z} = (z_1, z_2, ..., z_{nc})^T$, $\mathbf{d}$ is the vector of component molar densities in the trial phase, $\mathbf{d} = (d_1, d_2, ..., d_{nc})^T$, with

$$d_i = \frac{W_i}{V} = \frac{w_i}{v}; i = 1, nc \tag{5}$$

where $\mathbf{W} = (W_1, W_2, ..., W_{nc})^T$ are formally mole numbers in the trial phase and $\mathbf{d_z}$ is the vector of component molar densities in the feed (which are fixed, calculated only once at the beginning of iterations), with

$$d_{iz} = \frac{n_{iz}}{V_z} = \frac{z_i}{v_z}; i = 1, nc \tag{6}$$

The TPD function in Eq. (4) can be used for both PT (at pressure and temperature specifications) [36-38] and VTN (at volume, temperature and moles specifications) [39-42] phase stability testing. For PT stability, $P_z = P_{spec}$ and V_z is the root of the EoS $P(V_z, T_{spec}, \mathbf{n_z}) = P_{spec}$, corresponding to the minimum Gibbs free energy. For VTN stability, $V_z = V_{spec}$ and the pressure is calculated explicitly from the EoS $P_z = P(V_{spec}, T_{spec}, \mathbf{n_z})$.

The TPD function is minimized subject to the linear inequality constraint $c(\mathbf{d}) = \sum_{i=1}^{nc} b_i d_i - 1 < 0$ (equivalent to $v > b$) and to variable bounds $d_i \geq 0; i = 1, nc$.

The logarithm of the fugacity can be written as

$$\ln f_i(\mathbf{d}) = \ln d_i + \ln \Psi_i(\mathbf{d}) \tag{7}$$

where the density function was defined as [42]

$$\Psi_i(\mathbf{d}) = \frac{f_i(\mathbf{d})}{d_i} \tag{8}$$

and was chosen to isolate component molar densities d_i in the stationarity condition, Eq. (7).

The gradient vector is

$$g_i = \frac{\partial D}{\partial d_i} = \ln f_i(\mathbf{d}) - \ln f_{iz}(\mathbf{d_z}) = \delta_{ij} + \ln \Psi_i(\mathbf{d}) - \ln \Psi_{iz}(\mathbf{d_z}); i = 1, nc \tag{9}$$

the Hessian matrix is (taking into account Eq. 7)

$$H_{ij} = \frac{\partial^2 D}{\partial d_i \partial d_j} = \frac{\partial g_i}{\partial d_j} = \frac{\partial \ln f_i}{\partial d_j} = \frac{\delta_{ij}}{d_i} + \frac{\partial \ln \Psi_i}{\partial d_j}; i, j = 1, nc \tag{10}$$

and the Newton iteration equation is $\mathbf{H}\Delta\mathbf{d} = -\mathbf{g}$.

The diagonal term δ_{ij} / d_i in the ideal part of the Hessian matrix may span many orders of magnitude and can ruin the condition number, as explained and exemplified in Refs. [46-49].A proper scaling is thus required [47-49].

The change of variables $\alpha_i = 2\sqrt{d_i}$ (which follows from the scaling methodology of Nichita and Petitfrere [47] and is formally similar to Michelsen's [32] one) is suitable, since it replaces δ_{ij} / d_i with δ_{ij} on the main diagonal of the transformed Hessian matrix.

By using as independent variables α_i, the Newton iteration equation is

$$\mathbf{H}^* \Delta\boldsymbol{\alpha} = -\mathbf{g}^* \tag{11}$$

where the gradient is $\mathbf{g}^* = \mathbf{Tg}$, the Hessian is $\mathbf{H}^* = \mathbf{THT}$ and $\mathbf{T}$ is a diagonal transformation matrix of elements $T_{ij} = \delta_{ij}\sqrt{d_i}$. Thus, $g_i^* = \sqrt{d_i}\, g_i$ and $H_{ij}^* = \sqrt{d_i}\sqrt{d_j}\, H_{ij}$; details can be found in Refs. [42,48].

Several sets of independent variables were tested for both PT [38] and VTN [42] phase stability testing; the variables α_i proved to be, from far away, the best choice (with no failures or local increases in the number of iterations) among all tested variables. Moreover, our VTN phase stability testing was found to be 2-3 times faster than previous formulations [42].

4. Volume-based phase stability testing with capillary pressure

Recently, Kou and Sun [26] derived the phase stability conditions at VTN specifications with capillary pressure. At constant temperature, $T = T_{spec}$, the dimensionless TPD function in terms of component mole numbers and volume is

$$D_V(\mathbf{W},V) = \sum_{i=1}^{nc} W_i \left[\ln f_{iw}(\mathbf{W},V) - \ln f_{iz}(\mathbf{n_z},V_z)\right] - \frac{V\left[P_w(\mathbf{W},V) - P_z(\mathbf{n_z},V_z)\right]}{RT} + \gamma\frac{VP_C(\mathbf{W},V)}{RT} \tag{12}$$

the index *w* refers to the-trial phase.

A mixture is stable if the TPD function is non-negative for all possible values of **W** and *V* (its global minimum is zero).

The values of γ are $\gamma = -1$ if it is assumed that the reference phase is vapor and the trial phase is liquid ($P_z = P_V$ and $P_w = P_L$) and $\gamma = +1$ if it is assumed that the reference phase is liquid and the trial phase is vapor ($P_z = P_L$ and $P_w = P_V$). Clearly, if $\gamma = 0$, Eq. (12) corresponds to the bulk fluid.

The TPD function in Eq. (12) must be normalized either to unit mole numbers or to unit volume [38]. In the latter case, the TPD function in terms of component molar densities is (at $T = T_{spec}$) [26]

$$D(\mathbf{d}) = \sum_{i=1}^{nc} d_i \left[\ln f_{iw}(\mathbf{d}) - \ln f_{iz}(\mathbf{d_z})\right] - \frac{P_w(\mathbf{d}) - P_z(\mathbf{d_z})}{RT} + \gamma \frac{P_C(\mathbf{d})}{RT} \tag{13}$$

As mentioned earlier for the bulk case, the minimization of this function can be performed for both PT and VTN stability testing. In this work, all calculations are performed at pressure and temperature specifications.

The elements of the gradient vector are

$$g_i = \frac{\partial D}{\partial d_i} = \delta_{ij} + \ln \Psi_{iw}(\mathbf{d}) - \ln \Psi_{iz}(\mathbf{d_z}) + \frac{\gamma}{RT} \frac{\partial P_C(\mathbf{d})}{\partial d_i}; i = 1, nc \tag{14}$$

and the elements of the Hessian matrix are

$$H_{ij} = \frac{\partial^2 D}{\partial d_i \partial d_j} = \frac{\partial g_i}{\partial d_j} = \frac{\delta_{ij}}{d_i} + \frac{\partial \ln \Psi_{iw}(\mathbf{d})}{\partial d_j} + \frac{\gamma}{RT} \frac{\partial^2 P_C(\mathbf{d})}{\partial d_i \partial d_j}; i, j = 1, nc \tag{15}$$

The Newton iteration equation with molar densities as independent variables is

$$\mathbf{H}\Delta\mathbf{d} = -\mathbf{g} \tag{16}$$

The partial derivatives of the density function with respect to molar densities in Eq. (15) are given in Ref. [42].

Eq. (3) can be written as

$$\sigma^{1/E} = \sum_{i=1}^{nc} \Pi_i (d_{iL} - d_{iV}) \tag{17}$$

or further, for phase stability testing the interfacial tension is expressed as

$$\sigma(\mathbf{d}) = \left(\sum_{i=1}^{nc} \gamma \Pi_i (d_{iz} - d_i) \right)^E \tag{18}$$

Whichever the reference phase, vapor or liquid, Eq. (18) is equivalent to Eq. (17) for $\gamma = \pm 1$.

The first- and second-order partial derivatives of the capillary pressure with respect to component molar densities are

$$\frac{\partial P_C(\mathbf{d})}{\partial d_i} = -\gamma \frac{2\cos\theta}{r} E\ \Pi_i \sigma(\mathbf{d})^{\left(\frac{E-1}{E}\right)}; i = 1, nc \tag{19}$$

and

$$\frac{\partial^2 P_C(\mathbf{d})}{\partial d_i \partial d_j} = \frac{2\cos\theta}{r} E(E-1) \Pi_i\ \Pi_j \sigma(\mathbf{d})^{\left(\frac{E-2}{E}\right)}; i, j = 1, nc \tag{20}$$

Note that we need only partial derivatives with respect to component molar densities and, unlike in the conventional approach, no implicit functions are involved in the differentiation process.

The objective function, gradient vector and Hessian matrix with capillary pressure are related to those of the bulk fluid by

$$D^{(cap)}(\mathbf{d}) = D^{(bulk)}(\mathbf{d}) + \gamma a_D(\mathbf{d}) \tag{21a}$$

$$g_i^{(cap)}(\mathbf{d}) = g_i^{(bulk)}(\mathbf{d}) + \gamma a_G(\mathbf{d})\Pi_i \tag{21b}$$

$$H_{ij}^{(cap)}(\mathbf{d}) = H_{ij}^{(bulk)}(\mathbf{d}) + \gamma a_H(\mathbf{d})\Pi_i\,\Pi_j \tag{21c}$$

where the constants a_D, a_G and a_H are easily obtained by identification from Eqs. (13), (19) and (20), respectively; these additional terms (containing the capillary pressure and its first- and second order partial derivatives with respect to molar densities) depend only on component molar densities at specified temperature and fixed curvature radius and contact angle.

An examination of equations (21a) to (21c) suggests that their particular form has an immediate practical importance, that is, the proposed method can be easily implemented by modification of existing volume-based stability testing codes [38,42].

As in the bulk fluid case [38,42], the change of variables $\alpha_i = 2\sqrt{d_i}$ is used, and the linear system $\mathbf{H}^*\Delta\boldsymbol{\alpha} = -\mathbf{g}^*$ is solved, with $\mathbf{g}^* = \mathbf{Tg}$ and $\mathbf{H}^* = \mathbf{THT}$.

If the TPD function in Eq. (12) is normalized to unit mole numbers, an alternative volume-based formulation can be given with volume and mole numbers as variables, using a modified TPD function (similar to Nichita [38] for the bulk case) and leading to a system of *nc*+1 equations (equilibrium and capillary pressure equations) with *nc*+1 unknowns (mole numbers and volume); the number of equations is the same as in the conventional bulk case. Such an approach would require additional partial derivatives and have poorer condition numbers of the Hessian matrix [38]).

Extensive testing in the bulk fluid case showed that the formulation in molar densities (using the change of variables $\alpha_i = 2\sqrt{d_i}$), adopted in this work, performs globally better (it is faster and more reliable) than that in mole numbers and volume [38].

5. Solution Method

Robustness and computational speed are the main requirements for a computational algorithm. A reliable algorithm must be able to return the correct answer in all possible situations and deal with difficult, pathological ones. The most difficult domains for the phase stability problem are the neighborhoods of singularities, which correspond to saddle points of the objective function. The Hessian matrix is singular at the STLL [49,50] (for a non-trivial composition, with a positive value of the TPD function) and at the spinodal (for a trivial composition and the TPD function equal to zero; in this case, convergence problems are less severe than near the STLL). Exactly at a singularity (either STLL or spinodal), any gradient-based calculation method diverges; the number of iterations is increasing asymptotically as these points are approached [46,48,49]. Any algorithm must manage the case when the Hessian matrix has to cross a region of indefiniteness during iterations (such as outside the STLL in a PT plane), by guaranteeing a descent direction. A systematic increase in iteration numbers were also observed for the bulk fluid at low temperatures [38,42] (in both conventional and volume-based approaches).

In volume-based methods, unlike in conventional ones, the successive substitution method (very useful in early iteration stages before switching to Newton iterations) cannot be used [34,40,42] and thus robust modified Newton methods are required. A modified Cholesky factorization [51] (to ensure a descent direction if some eigenvalues of the Hessian matrix are negative; the Schnabel and Eskow [52,53] version is implemented) and a two-stage line search procedure (to ensure that iterates remain in the feasible domain and the objective function is decreased at each iteration) are used in Newton iterations. The calculation protocol was described in detail in our previous work on volume-based methods [38,42,54,55]. Without the modified Cholesky factorization (or other methods capable to deal with possible non-positive-definiteness of the Hessian matrix during iterations) the algorithm is not robust and hundreds of iterations may be required for convergence or divergence may occur, especially at some points outside (in a P-T plane) the STLL [49], or even in the two-phase region at low temperatures [42]. The robustness is strengthened by the change of variables. For bulk VTN phase stability, the approach turns out to be significantly faster than previous formulations [42].

It should be noted that even though the optimization problem is a bound- and linear inequality- constrained minimization of the TPD function with respect to component molar densities, methods specific to unconstrained optimization are used and the line search procedure ensures that the constraints are not violated during iterations.

The two-sided Michelsen's [32] initialization scheme is used in this work for two-phase systems (in a multiphase context, more elaborate initialization schemes such as the ones proposed by

Li and Firoozabadi [56] or Castier [41] must be used). At pressure and temperature specifications, Wilson's correlation for ideal equilibrium constants [57] is used to generate initial estimates of the formal mole numbers in the trial phase

$$K_i^{(0)} = \frac{P_{ci}}{P} \exp\left[5.373(1+\omega_i)(1-T_{ci}/T)\right] \tag{22}$$

The initial guesses of trial phase formal mole numbers are

$$W_i^{(0)} = z_i K_i^{(0)} \tag{23a}$$

for a liquid-like mixture (trial phase is vapor-like; this initialization is denoted as type L) and

$$W_i^{(0)} = \frac{z_i}{K_i^{(0)}} \tag{23b}$$

for a vapor-like mixture (trial phase is liquid-like; this initialization is denoted as type V).

The initial guess for the volume $V^{(0)}$ is obtained by solving for volume the implicit form of the EoS at specified pressure, temperature and mole numbers of the trial phase. If the cubic EoS has three real roots, the root corresponding to the smallest Gibbs free energy of the trial phase is selected. The initial values of the molar densities are $d_i^{(0)} = W_i^{(0)} / V^{(0)}$.

For a two-phase system, the TPD value at stationary points changes sign on an isotherm at the spinodal if $T < T_c$ and at the dew point pressure if $T > T_c$ for a type V initialization and at the bubble point pressure if $T < T_c$ and at the spinodal if $T > T_c$ for a type L initialization. The TPD function exhibits a discontinuity at the STLL if $T > T_c$ for a type V initialization and if $T < T_c$ for a type L initialization [38].

At volume, temperature and moles specifications (VTN stability), the initialization scheme of Mikyška and Firoozabadi [40], as slightly modified by Nichita [42] (to use Wilson's [57] K-values) can be used.

Iterations are stopped when $S_g < \varepsilon_g$ or $S_\Delta < \varepsilon_\Delta$, in which

$$S_g = \left(\sum_{i=1}^{nc} g_i^2 \right)^{1/2} \tag{24}$$

is the Euclidian norm of the gradient vector and

$$S_\Delta = \left(\sum_{i=1}^{nc} (\Delta\alpha_i)^2 \right)^{1/2} \tag{25}$$

is the Euclidian norm of the direction vector, with $(\Delta\alpha_i)^{(k)} = \alpha_i^{(k+1)} - \alpha_i^{(k)}$; in this work $\varepsilon_g = 10^{-10}$ and $\varepsilon_\Delta = 10^{-7}$. The maximum number of iterations is set to 200.

The required thermodynamic functions (fugacity and pressure) and their partial derivatives are usually expressed (and coded in phase equilibrium packages and simulators) in terms of mole numbers, volume and temperature, while here we need their dependence on component molar densities and temperature. Of course, $\ln f_i$ and P can be rewritten in terms of molar densities (as given in Refs. [37,39] for cubic EoS), but it is more convenient to use homogeneity properties to obtain

$$\ln f_i(\mathbf{d},T) = \ln f_i(\mathbf{n},V,T); i = 1, nc \tag{26}$$

$$P(\mathbf{d},T) = P(\mathbf{n},V,T) \tag{27}$$

and

$$\frac{\partial \ln f_i(\mathbf{d},T)}{\partial d_j} = V \frac{\partial \ln f_i(\mathbf{n},V,T)}{\partial n_j}; i, j = 1, nc \tag{28}$$

as explained in Refs. [38,42] (the above relations are valid for any EoS).

The expressions of $\ln f_i(\mathbf{n},V,T)$, $\partial \ln f_i(\mathbf{n},V,T)/\partial n_j$ (having a very simple form) and $P(\mathbf{n},V,T)$ for a general form of two-parameter cubic EoS can be found in Refs. [38,42,54,55]. Any existing routine calculating these quantities from any pressure-explicit EoS can be used in the proposed approach.

6. Results and discussion

Numerical experiments have been carried out for two mixtures using a general form of two-parameter cubic EoS, including the Soave-Redlich-Kwong (SRK) EoS [58] and the Peng-Robinson (PR) EoS [59,60]. A zero contact angle is considered ($\cos\theta = 1$) and the scaling factor in the Weignaud-Katz expression for the interfacial tension is $E = 4$.

Volume-based Newton iterations with modified Cholesky factorization and a two-stage line search procedure using the independent variables $\alpha_i = 2\sqrt{d_i}$ are used in stability testing with capillary pressure (see previous section). The code from Ref. [42] was modified to account for capillary pressure influence. In the conventional method, the SSI method with lagged update of the pressure in the trial phase (P_w) is used and the results are taken as a basis of comparison. Saturation

pressures are located by tracking sign changes in the TPD functions, then refining up to the desired accuracy. STLLs are located by recording the limit of positive non-trivial values of the TPD function in the single phase region.

The first test mixture is an oil from Sherafati and Jessen [9], described by 15 components, denoted here SJ15. The SRK EoS is used; composition, component properties (including parachors) and non-zero binary interaction parameters (BIPs) are taken from Ref. [9].

The phase envelopes of the SJ15 oil are plotted in **Fig. 1a** for the bulk fluid (P_{sat}) and with capillary pressure (P_z) (r=10 nm), obtained using both the conventional approach and the volume-based minimization (the two STLLs are also drawn, exhibiting different shapes, as well as the spinodal curve and the critical point at T_c=721.15 K and P_c=114.67 bar); the pressures of the trial phase (P_W) are also plotted. The spinodal is obviously the same for the bulk fluid and with capillary pressure (if $\mathbf{d} = \mathbf{d}_z$ all terms are vanishing in Eq. 13). For the bulk fluid and the conventional method with capillary pressure, the results are essentially the same as those reported in Ref. [9]. **Fig. 1b** shows a detail around the cricondentherm points. The differences between conventional and volume-based approaches are minor, except at high temperatures: the cricondentherm point is shifted by 9 K in the conventional approach and by 16 K in the volume-based minimization. The shift towards higher temperatures of the cricondentherm points of confined mixtures as compared to the bulk fluid was previously reported in Refs. [5-10].

Phase stability calculations are performed for the SJ15 oil on three isotherms (marked with dashed lines in Fig. 1a), T=338.15 K, T=700 K and T=800 K. A type L initialization is used for the first two temperatures (on the bubble point side) and a type V initialization is used for the third one (on the dew point side).

The TPD functions (for the bulk fluid and with capillary pressure, using both conventional and volume-based methods) vs. pressure are plotted in **Fig. 2** at T=338.15 K. Intersections with the abscissae give the location of the saturation pressures. The conventional and volume-based STLLs are different in both bulk (see Ref. [38]) and capillary pressure cases.

The number of Newton iterations in the volume-based approach at T=383.15 K, without and with capillary pressure, are plotted against pressure in **Fig. 3**. The locations of saturation pressures are marked in **Fig. 3** (and also in all subsequent figures presenting the number of iterations) with a dotted line (bulk fluid), a dashed line (conventional with capillary pressure) and a dash-dotted line (volume-based method with capillary pressure). The locations of the STLLs are indicated by peaks in the

number of iterations. Sherafati and Jessen [9] reported for this temperature and for 1 bar below the saturation pressure 5 iterations for the fully implicit method and 8 iterations for the Newton method with lagged P_w update; at the same conditions, 7 Newton iterations are required in this work at the same conditions.

The variations of the Euclidean norms during iterations (starting from type L initialization) are depicted in **Fig. 4** (the tolerance in the convergence criterion is marked with a dashed line) for several pressures at T=383.15 K (r=10 nm). As expected, the convergence is quadratic near the solution; however, in some cases the gradient norm increases (although the objective function is slowly decreasing); the explanation for this behavior and calculation examples can be found in Refs. [46,49].

The condition numbers of Hessian matrices at the stationary points (obtained from a type L initialization) for the variables d_i and α_i, at T=383.15 K are plotted in **Fig. 5**; normal peaks at singularities are observed in both cases, but condition numbers are significantly different, from 6 to 12 orders of magnitude in the interval between the spinodal and the STLL. For these particular conditions, capillary pressures slightly improve condition numbers for d_i variables. The importance of scaling was discussed earlier [38, 42,46-48]; for instance, in bulk phase stability testing, failures were reported with d_i variables (at VTN [40,42] and PT [38] stability), while no failures occurred at the same conditions using the α_i variables [38,42].

Fig. 6 gives the number of volume-based Newton iterations (bulk fluid and with capillary pressure for r=10 nm) vs. pressure at T=700 K. In this case, conditions are close to the critical point and saturation (bubble point) pressures are very close for bulk and capillary in both conventional and volume-based stability. Sherafati and Jessen [9] reported for this temperature and for 1 bar below the saturation pressure 10 iterations for the fully implicit method and 9 iterations for Newton iterations with lagged P_w update; at the same conditions, 11 Newton iterations are required in this work (volume-based methods are slightly slower than conventional ones in terms of number of iterations, as shown recently [42,54], but it must be remembered that a volume-based iteration is faster, since the EoS is not solved and partial derivatives are simpler).

For the volume-based approach, the Euclidean norms during iterations are plotted in **Fig. 7**.at various pressures for the SJ15 oil at T=700 K (bulk fluid and with capillary pressure for r=10 nm). Again, quadratic convergence is observed near the solution; at P=121.8 bar (just above the STLL), the gradient norm increases after 10 iterations and rapid convergence is restored after only a diagonal correction of the Hessian matrix.

The number of volume-based Newton iterations (bulk fluid and with capillary pressure for r=10 nm) are plotted vs. pressure at T=800 K (close to the cricondentherm point of the bulk fluid) in **Fig. 8**. Similar convergence behavior and small differences in the number of iterations are observed in the two considered situations.

The second test mixture (Y8 mixture, Yarborough [61]) is a six-component synthetic model gas condensate containing normal-alkanes. The PR EoS is used, with composition and component properties (taken from Reid et al. [62]) listed in **Table 1**; all BIPs are equal to zero. The parachors are taken from Escobedo and Mansoori [63].

The phase envelopes (bulk fluid and with capillary pressure for r=10 nm) of the Y8 mixture are plotted in **Fig. 9a**, showing also the pressures of the trial phase (P_W), the STLL, the spinodal curve and the critical point at T_c=291.65 K and P_c=211.09 bar.

The differences between the conventional approach and the volume-based minimization are small for this mixture, as shown in **Fig. 9b** presenting a detail around the cricondentherm points, which are shifted with about 3 K in both conventional approach and volume-based minimization.

The number of volume-based Newton iterations (without and with capillary pressure for r=10 nm) are plotted vs. pressure in **Fig. 10** for the Y8 mixture at T=435 K (close to the cricondentherm point of the bulk).

Phase stability testing calculations using the volume-based method including capillary pressure are performed (with r=10 nm) for a large number of points in the P-T plane for both SJ15 oil and Y8 mixtures. The boxes in the T-P plane are defined by [200 K, 900 K] and [1 bar, 300 bar], with increments $\Delta P = 1$ bar and $\Delta T = 1$ K, giving 209,300 points for the SJ15 oil and [150 K, 600 K] and [1 bar, 300 bar], with increments $\Delta P = 1$ bar and $\Delta T = 1$ K, giving 134,550 points for the Y8 mixture.

The average numbers of iterations are given in **Table 2** for the SJ15 oil (ranging from about 10 to 15) and for the Y8 gas condensate (ranging from about 8 to 11). The maximum number of iterations is set to 200, but for the test examples 30 iterations are exceeded for very few points and there was not any failure.

For both mixtures, a relatively large number of iterations is required at low temperatures for the entire pressure range for the type V initialization. Note however that at low temperatures the natural stability test for mixtures is that of a liquid phase (from a type L initialization); both cases are given to show the capability of the proposed method to handle different situations. If smaller P-T windows are taken by increasing the lower bound of temperature intervals (a temperature range [300 K, 900 K], giving 179,400 points for the SJ15 oil and a temperature range [250 K, 600 K], as in Ref.

[38], giving 104,650 points for the Y8 mixture), the average number of iterations in a type V initialization is decreased by more than two for both the SJ15 oil and Y8 mixtures. The average number of iterations for the restricted boxes is given for each case in brackets in **Table 2**.

The proposed method is robust (no failures recorded) and fast (except at low temperatures, where it is reasonably fast). Globally, very small differences are observed between the number of iterations in stability testing with/without capillary pressure (as also suggested earlier by Figs. 3, 8 and 10).

The number of iterations required in stability testing with capillary pressure (for r=10 nm) in the T-P plane are plotted in **Fig. 11** (type V initialization) and **Fig. 12** (type L initialization) for the SJ15 oil and in **Fig. 13** (type V initialization) and **Fig. 14** (type L initialization) for the Y8 mixture. The increase in the numbers of iterations near the STLL (at $T > T_c$, type V initialization and $T < T_c$, type L initialization) and the spinodal (at $T < T_c$, type V initialization and $T > T_c$, type L initialization) can be clearly observed in Figs. 11 to 14.

In order to study the influence of the capillary radius on phase boundaries, capillary radii are varied down to r=5 nm (considered the limit of viability of the parachor model [30]). For the bulk fluid and for several capillary radii, the phase envelopes (constructed using the volume-based method) of the SJ15 oil are drawn in **Fig. 15** and those of the Y8 mixture are drawn in **Fig. 16**. The shift in the cricondentherm point at r=5 nm is important for the SJ15 oil, about 47 K and of 8 K for the Y8 mixture.

The influence of capillary radius on saturation pressure at a given temperature using both conventional and volume-based approaches is given for the SJ15 Oil at T=383.15 K (on the bubble point side) in **Fig. 17** and for the Y8 mixture at T=435 K (on the dew point side, close to the cricondentherm) in **Fig. 18** (showing both retrograde and lower dew points). The differences between the results of conventional and volume-based minimization approaches (which naturally increase when the capillary radii are decreasing) are important only at high temperatures and at very low temperatures. For r>20 nm there is practically no difference, for r=5-10 nm the differences are small. At a very low capillary radius of r=3 nm (at which the parachor model is no more valid [30], included here to test the capability of the method to handle such situations), the differences become more important.

As mentioned before, in conventional methods the solution does not correspond to a minimization, leading to a non-symmetric Jacobian matrix, because the equilibrium equations are not

stationarity conditions for the TPD function if the dependence $P_w = P_w(\mathbf{W})$ is not taken into account in the differentiation to obtain the gradient vector.

If a minimization of the TPD function is used instead of solving together the gradient of the bulk fluid with the capillary pressure equation: i) the results are (generally slightly) different, ii) the differences are more important on the dew point side than on the bubble point side (where notable differences are only at low temperatures), iii) the differences increase with decreasing the capillary radius, iv) the shift of cricondenterm points toward higher temperatures is more pronounced. The shape of phase envelopes and the trends are the same in both cases, showing a suppression of bubble point pressures, inflated phase envelopes on the dew point side and a shift towards higher temperatures of the cricondentherm points of confined mixtures as compared to the bulk fluid.

Whether to consider in the conventional approach the full minimization of the TPD function (by considering the dependence of the pressure in the trial phase on composition via the capillary pressure equation in the zero-gradient equation) instead of solving together the equilibrium and capillary pressure equations is a problem not yet addressed and is currently under investigation.

The formalism presented here is valid for volume-based stability testing including capillary pressure at pressure and temperature specifications and at temperature, volume and moles specifications (for the pressure in the reference phase calculated explicitly from the EoS at specifications). The volume-based stability testing procedure is not model-dependent: any pressure-explicit EoS and any interfacial tension model explicit in volume and mole numbers can be used.

In this work, a constant capillary radius is considered, as in most of the papers in the literature. However, in realistic situations (e.g. fluids in porous media) the capillary radius is dependent on saturation states (as for the classical Leverett J-function) and on pore size distribution; these aspects are intended to be addressed in a future work.

The proposed method for volume-based stability testing is much simpler than the evolutionary method of Kou and Sun [26] and easily applicable for mixtures with many components. It was applied over wide temperature and pressure ranges, with the construction of the entire phase envelope and STLL. The proposed method is also simpler than conventional methods (the EoS is not solved for volume, the required partial derivatives are simpler and there is no need to a lagged update which lowers the degree of implicitness). The proposed method is easily implemented by simple modifications of robust and efficient existing codes for VTN or volume-base PT phase stability testing [38,42].

In the proposed formulation, the numbers of iterations with/without capillary pressure are very close and the convergence behavior is similar in both cases. As compared to the bulk fluid case, neither robustness nor efficiency is affected by including the capillary pressure terms. The robustness and computational speed recommend the proposed method for phase stability testing with capillary pressure to be used in compositional reservoir simulation of unconventional reservoirs.

7. Conclusions

A volume-based method is proposed for phase stability testing including capillary pressure. The TPD function is minimized with respect to component molar densities. The optimization problem is a bound and linear inequality constrained one. A modified Cholesky factorization ensures descent directions, a two-stage line search procedure is used to prevent constraints violations and to ensure that the objective function is decreased during iterations and a proper scaling enforces robustness.

The EoS must not be solved for volume and the required partial derivatives are simpler than in conventional phase equilibrium calculations. The calculation framework is not dependent on the thermodynamic model and any pressure-explicit equation of state can be used. The Weinaug-Katz model is used for interfacial tensions (any expression in which the interfacial tension is explicit in component molar densities can be used) and the additional partial derivatives (contained in terms related to capillarity) in the gradient vector and Hessian matrix have very simple expressions, as compared to the conventional formulation.

Unlike in conventional phase stability testing including capillary pressure, a minimization problem is solved, thus full advantage is taken of symmetry in building the Hessian matrix, solving the linear system and ensuring descent directions. To the best of our knowledge, this is the first time that the phase stability testing including capillary pressure is solved by direct minimization of the TPD function using a volume-based approach.

The proposed method is attractive because of its simplicity, the easiness to modify existing codes to include capillary pressure effects, its robustness and efficiency.

Acknowledgements

This paper was first presented at the 30th European Symposium of Applied Thermodynamics (ESAT), held in Prague on June10-13, 2018.

List of symbols

D_V	TPD function in terms of mole numbers and volume
D	TPD function in terms of molar densities
D^*	Michelsen's modified TPD function
d_i	molar density of component i (trial phase)
d_{iz}	molar density of component i (feed)
E	scaling exponent
f_i	fugacity of component i
$\mathbf{g}$	gradient vector; minimization with respect to d_i
$\mathbf{g}^*$	gradient vector; minimization with respect to α_i
g_i	elements of the gradient vector
$\mathbf{H}$	Hessian matrix
H_{ij}	elements of the Hessian matrix
$\mathbf{H}^*$	Hessian matrix; minimization with respect to α_i
$\mathbf{J}$	Jacobian matrix
K_i	equilibrium constants
nc	number of components
n_{iz}	mole numbers of component i in the feed
P	pressure
P_C	capillary pressure
P_w	trial phase pressure
P_z	reference phase pressure
R	universal gas constant
r	curvature radius
T	temperature
$\mathbf{T}$	transformation matrix
V	volume
v	molar volume
w_i	mole fraction of component i in the trial phase
W_i	mole numbers of component i in the trial phase
x_i	mole fraction of component i in the liquid phase
y_i	mole fraction of component i in the vapor phase
z_i	feed composition

Greek letters

α_i	variables for stability testing
γ	±1, depending on the reference phase
δ_{ij}	Kronecker delta
ε	tolerance for convergence

φ_i	fugacity coefficient of component *i*
σ	interfacial tension
ρ	mixture molar density
θ	contact angle
ξ_i	independent variables
Ψ_i	density function of component *i*
ω	acentric factor
Π_i	Parachor of component *i*

Subscripts

i,j	component index
C	capillary
c	critical
L	liquid
spec	specification
V	vapor
w	trial phase
z	reference phase

Superscripts

(*k*)	iteration level
(0)	at initial guess

References

[1] P.M. Sigmund, P.M. Dranchuk, N.R. Morrow, R.A. Purvis, Retrograde Condensation in Porous Media, Soc. Petrol. Eng. J. 13 (1973) 93-104.

[2] A. Danesh, D. Krinis, G.D. Henderson, J.M. Peden, Visual Investigation of Retrograde Phenomena and Gas Condensate Flow in Porous Media, Rev. Inst. Fr. Pét. 45 (1990) 79-87.

[3] R. Tindy, M. Raynal, Are test-cell saturation pressures accurate enough? Oil Gas J. 34 (1966) 126-129.

[4] A. Shapiro, E.H. Stenby, Kelvin equation for a non-ideal multicomponent mixture, Fluid Phase Equilib. 134 (1997) 87-101.

[5] A. Shapiro, E.H. Stenby, Thermodynamics of the multicomponent vapor - liquid equilibrium under capillary pressure difference. Fluid Phase Equilib. 178 (2001) 17-32.

[6] A.I. Brusilovsky, Mathematical simulation of phase behavior of natural multicomponent systems at high pressures with an equation of state, SPE Reservoir Eng. 7 (1992) 117-122.

[7] D.R. Sandoval, W. Yan, M.L. Michelsen, The phase envelope of multicomponent mixtures in the presence of a capillary pressure difference, Ind. Eng. Chem. Res. 55 (2016) 6530-6538.

[8] E. Barsotti, S.P. Tan, S. Saraji, M. Piri, J.H. Chen, A review on capillary condensation in nanoporous media: Implications for hydrocarbon recovery from tight reservoirs, Fuel 184 (2016) 344-361.

[9] M. Sherafati, K. Jessen, Stability analysis for multicomponent mixtures including capillary pressure, Fluid Phase Equilib. 433 (2017) 56-66.

[10] S.P. Tan, M. Piri, Retrograde behavior revisited: implications for confined fluid phase equilibria in nanopores, Phys. Chem. Chem. Phys. 19 (2017) 18890-18901.

[11] S.S. Neshat, R. Okuno, G.A. Pope, A Rigorous Solution to the Problem of Phase Behavior in Unconventional Formations With High Capillary Pressure, SPE J. 23 (2018) 1438-1451.

[12] Z. Jin, Bubble/dew point and hysteresis of hydrocarbons in nanopores from molecular perspective, Fluid Phase Equilib. 458 (2018) 177-185.

[13] B. Nojabaei, R.T. Johns, L. Chu, Effect of Capillary Pressure on Phase Behavior in Tight Rocks and Shales, SPE Reservoir Eval. Eng. 16 (2013) 281-289.

[14] J. Pang, J. Zuo, D. Zhang, L. Du, Effect of Porous Media on Saturation Pressures of Shale Gas and Shale Oil, IPTC-16419-MS, International Petroleum Technology Conference, 26-28 March, Beijing, China, 2013. DOI: 10.2523/IPTC-16419-MS

[15] B. Li, A.G. Mezzatesta, H.F. Thern, H. Zhang, J. Wu, B. Zhang, The Condition of Capillary Condensation and Its Effects on Gas-In-Place of Unconventional Gas Condensate Reservoirs, SPE 170837-MS, SPE Annual Technical Conference and Exhibition, 27-29 October, Amsterdam, The Netherlands, 2014. DOI: 10.2118/170837-MS

[16] T.W. Teklu, N. Alharthy, H. Kazemi, X. Yin, R.M. Graves, A.M. AlSumaiti, Phase Behavior and Minimum Miscibility Pressure in Nanopores, SPE Reservoir Eval. Eng. 17 (2014) 396-403.

[17] H. Sun, H.A. Li, A New Three-Phase Flash Algorithm Considering Capillary Pressure in a Confined Space, Chem. Eng. Sci. 193 (2019) 346-363.

[18] S.P. Tan, M. Piri, Equation-of-state modeling of confined-fluid phase equilibria in nanopores, Fluid Phase Equilib. 393 (2015) 48-63.

[19] Z. Jin, A. Firoozabadi, Thermodynamic Modeling of Phase Behavior in Shale Media, SPE J. 21 (2016) 190-207.

[20] B. Yan, Y. Wang, J.E. Killough, A fully compositional model considering the effect of nanopores in tight oil reservoirs, J. Petrol. Sci. Eng. 152 (2017) 675-682.

[21] N. Siripatrachai, T. Ertekin, R.T. Johns, Compositional Simulation of Hydraulically Fractured Tight Formation Considering the Effect of Capillary Pressure on Phase Behavior, SPE J. 22 (2017) 1046-1063.

[22] Y. Zhang, H.R. Lashgari, Y. Di, K. Sepehrnoori, Capillary pressure effect on phase behavior of CO_2/hydrocarbons in unconventional reservoirs, Fuel 197 (2017) 575–582.

[23] J.Y. Zuo , X. Guo, Y. Liu, S. Pan, J. Canas, O.C. Mullins, Impact of Capillary Pressure and Nanopore Confinement on Phase Behaviors of Shale Gas and Oil, Energy Fuels 32 (2018) 4705-4714.

[24] S.S. Neshat, R. Okuno, G.A. Pope, Simulation of Water and Condensate Blockage and Solvent Treatments in Tight Formations Using Coupled Three-Phase Flash and Capillary Pressure Models, SPE J 23 (2018) 1-14.

[25] M. Rezaveisi, K. Sepehrnoori, G.A. Pope, R.T. Johns, Thermodynamic Analysis of Phase Behavior at High Capillary Pressure, SPE J. 23 (2018) 1-14. https://doi.org/10.2118/175135-PA.

[26] J. Kou, S. Sun, A stable algorithm for calculating phase equilibria with capillarity at specified moles, volume and temperature using a dynamic model, Fluid Phase Equilib. 456 (2018) 7-24.

[27] L. Travalloni, M. Castier, F. W. Tavares, S.I. Sandler, Thermodynamic modeling of confined fluids using an extension of the generalized van der Waals theory, Chem. Eng. Sci. 65 (2010) 3088-3099.

[28] L. Travalloni, M. Castier, F.W. Tavares, Phase equilibrium of fluids confined in porous media from an extended Peng–Robinson equation of state, Fluid Phase Equilib. 362 (2014) 335-341.

[29] D.R. Sandoval, W. Yan, M.L. Michelsen, E.H. Stenby, Influence of Adsorption and Capillary Pressure on Phase Equilibria inside Shale Reservoirs, Energy Fuels, 32 (2018) 2819–2833.

[30] E. Santiso, A. Firoozabadi, Curvature dependency of surface tension in multicomponent systems, AIChE J. 52 (2006) 311-322.

[31] K.S.W. Sing, R.T. Williams, Historical aspects of capillarity and capillary condensation, Micropor. Mesopor. Mat. 154 (2012) 16-18.

[32] M.L. Michelsen, The isothermal flash problem. Part I. Stability, Fluid Phase Equilib. 9 (1982) 1-20.

[33] M.L. Michelsen, The isothermal flash problem. Part II. Phase split calculation, Fluid Phase Equilib. 9 (1982) 21-40.

[34] M.L. Michelsen, State function based flash specifications, Fluid Phase Equilib. 158-160 (1999) 617-626.

[35] U.K. Deiters, T. Kraska, High-Pressure Fluid Phase Equilibria: Phenomenology and Computation, Vol. 2, 1st Edition, Elsevier, Oxford, 2012. (pp.142-150)

[36] N.R. Nagarajan, A.S. Cullik, A. Griewank, New strategy for phase equilibrium and critical point calculations by thermodynamic energy analysis. Part I. Stability analysis and flash, Fluid Phase Equilib. 62 (1991) 191-210.

[37] D.V. Nichita, C. Duran-Valencia, S. Gomez, Volume-based thermodynamics global phase stability analysis, Chem. Eng. Commun. 193 (2006) 1194-1216.

[38] D.V. Nichita, Volume-based phase stability testing at pressure and temperature specifications, Fluid Phase Equilib. 458 (2018) 123-141.

[39] D.V. Nichita, J.C. de Hemptinne, S. Gomez, Isochoric phase stability testing for hydrocarbon mixtures, Petrol. Sci. Technol. 27 (2009) 2177–2191.

[40] J. Mikyška, A. Firoozabadi, Investigation of mixture stability at given volume, temperature, and number of moles, Fluid Phase Equilib. 321 (2012), 1-9.

[41] M. Castier, Helmholtz function-based global phase stability test and its link to the isothermal-isochoric flash problem, Fluid Phase Equilib. 379 (2014) 104-111.

[42] D.V. Nichita, Fast and robust phase stability testing at isothermal-isochoric conditions, Fluid Phase Equilib. 447 (2017) 107-124.

[43] C.F. Weinaug, D.L. Katz, Surface tensions of methane-propane mixtures, Ind. Eng. Chem. 35 (1943) 239-246.

[44] D.B. Macleod, On a relation between surface tension and density, Trans. Faraday Soc. 19 (1923) 38–41.

[45] S. Sugden, A relation between surface tension, density, and chemical composition, J. Chem. Soc., Trans. 125 (1924) 1177.

[46] M. Petitfrère, D.V. Nichita, Robust and efficient Trust-Region based stability analysis and multiphase flash calculations, Fluid Phase Equilib. 362 (2014) 51-68.

[47] D.V. Nichita, M. Petitfrere, Phase equilibrium calculations with quasi-Newton methods, Fluid Phase Equilib. 406 (2015) 194-208.

[48] M. Petitfrère, D.V. Nichita, A comparison of conventional and reduction approaches for phase equilibrium calculations, Fluid Phase Equilib. 386 (2015) 30-46.

[49] D.V. Nichita, Phase stability testing near the stability test limit, Fluid Phase Equilib. 426 (2016) 25-36.

[50] D.V. Nichita, D. Broseta, F. Montel, Calculation of convergence pressure/temperature and stability test limit loci of mixtures with cubic equations of state, Fluid Phase Equilib. 261 (2007) 176-184.

[51] P.E. Gill, W. Murray, Newton type methods for unconstrained and linearly constrained optimization. Math. Program. 7 (1974) 311-350.

[52] R.B. Schnabel, E. Eskow, A New Modified Cholesky Factorization, SIAM J. Sci. Stat. Comput. 11 (1990) 1136-1158.

[53] R.B. Schnabel, E. Eskow, A revised modified Cholesky factorization algorithm, SIAM J. Optim. 9 (1999) 1135-1148.

[54] D.V. Nichita, A volume-based approach to phase equilibrium calculations at pressure and temperature specifications, Fluid Phase Equilib. 461 (2018) 70-83.

[55] D.V. Nichita, New unconstrained minimization methods for robust flash calculations at temperature, volume and moles specifications, Fluid Phase Equilib. 466 (2018) 31-47.

[56] Z. Li, A.Firoozabadi, General Stategy for Stability Testing and Phase-split Calculations in Two and Three Phases. SPE J. 17 (2012) 1096-1107.

[57] G. Wilson, A modified Redlich-Kwong equation of state, application to general physical data calculations, the AIChE 65th National Meeting, Cleveland, Ohio, May 4-7, 1969.

[58] G. Soave, Equilibrium constants from a modified Redlich-Kwong equation of state. Chem. Eng. Sci. 27 (1972) 1197-1203.

[59] D.Y. Peng, D.B. Robinson, A new two-constant equation of state. Ind. Eng. Chem. Fund. 15 (1976) 59-64.

[60] D.B. Robinson, D.Y. Peng, 1978, The characterization of the heptanes and heavier fractions for the GPA Peng-Robinson programs, Gas Processors Association, Research Report RR-28.

[61] L. Yarborough, Vapor-Liquid Equilibrium Data for Multicomponent Mixtures Containing Hydrocarbon and Non-Hydrocarbon Components, J. Chem. Eng. Data 17 (1972) 129-133.

[62] R.C. Reid, J.M. Prausnitz, B.E. Poling, The Properties of Gases and Liquids, McGraw-Hill, Singapore, 1988.

[63] J. Escobedo, G.A. Mansoori, Surface tension prediction for pure fluids, AIChE J. 42 (1996) 1425-1433.

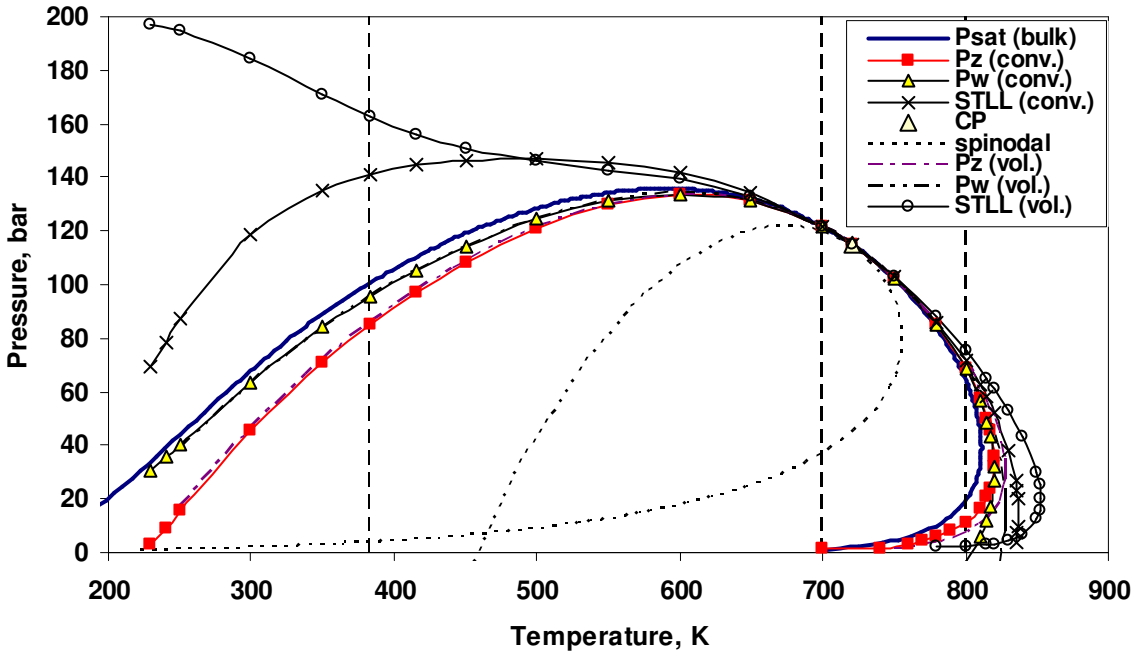

Fig. 1a Phase envelopes of the SJ15 oil, r=10 nm

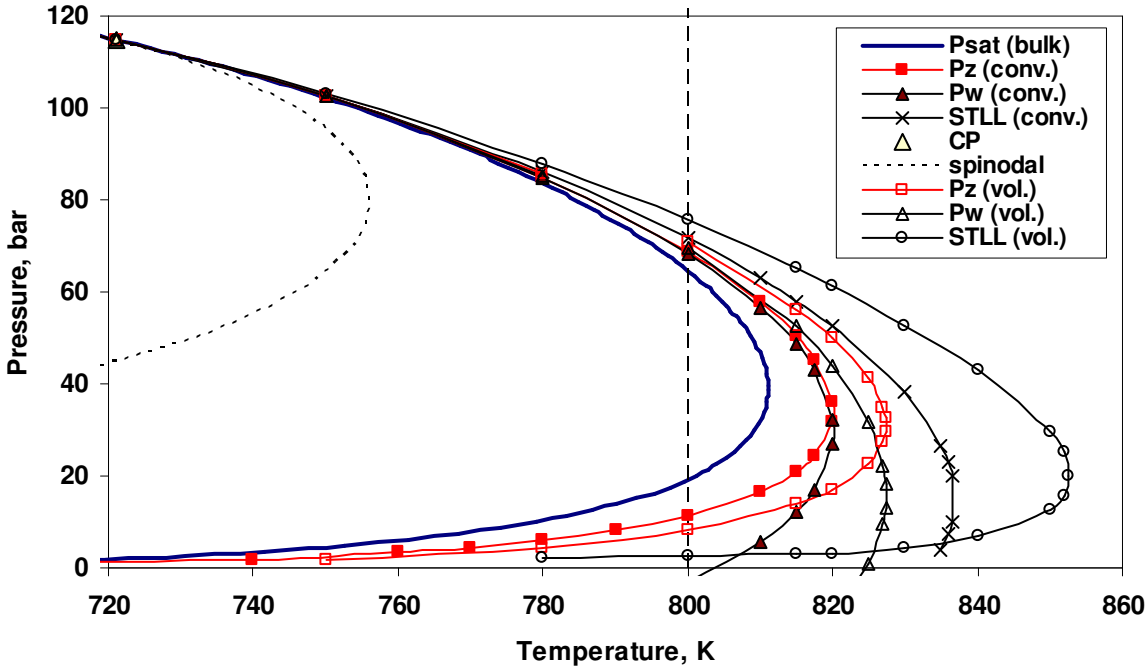

Fig. 1b Phase envelopes of the SJ15 oil, r=10 nm (detail)

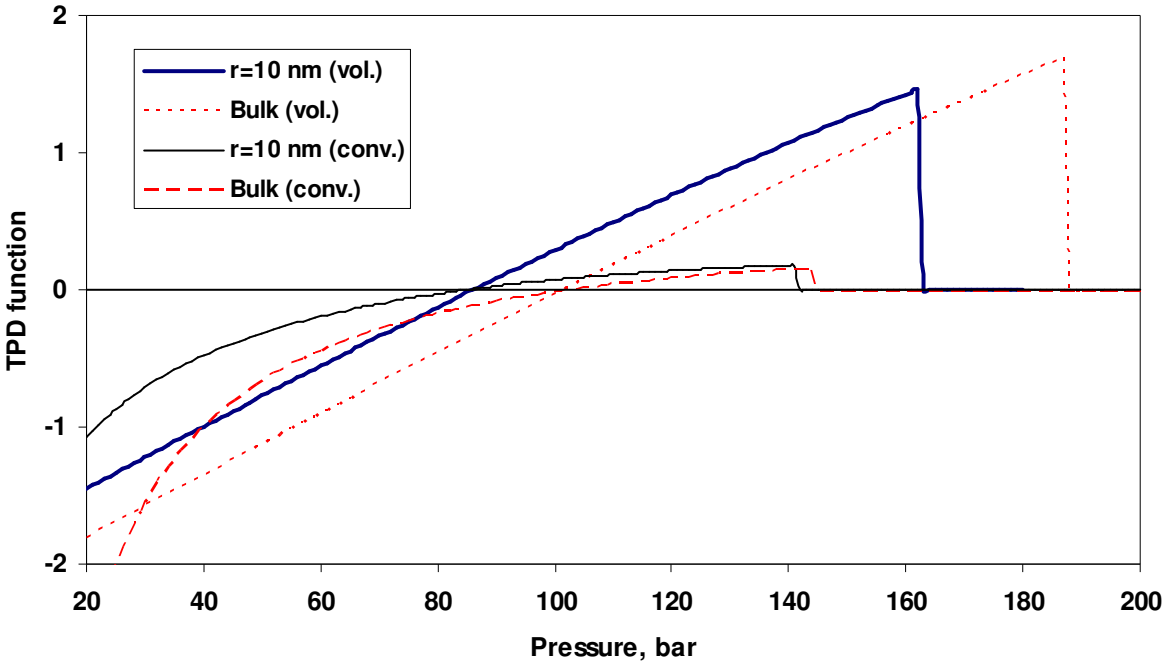

Fig. 2 TPD functions vs. pressure; SJ15 Oil at T=383.15 K (type L initialization)

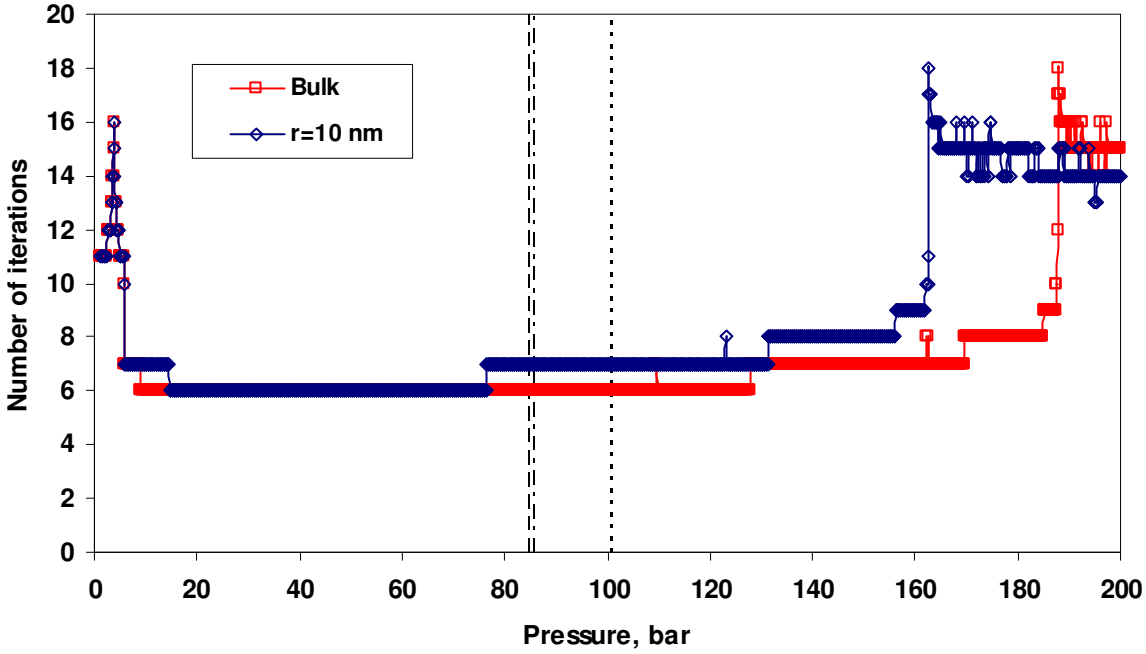

Fig. 3 Number of iterations vs. pressure; SJ15 Oil at T=383.15 K (type L initialization)

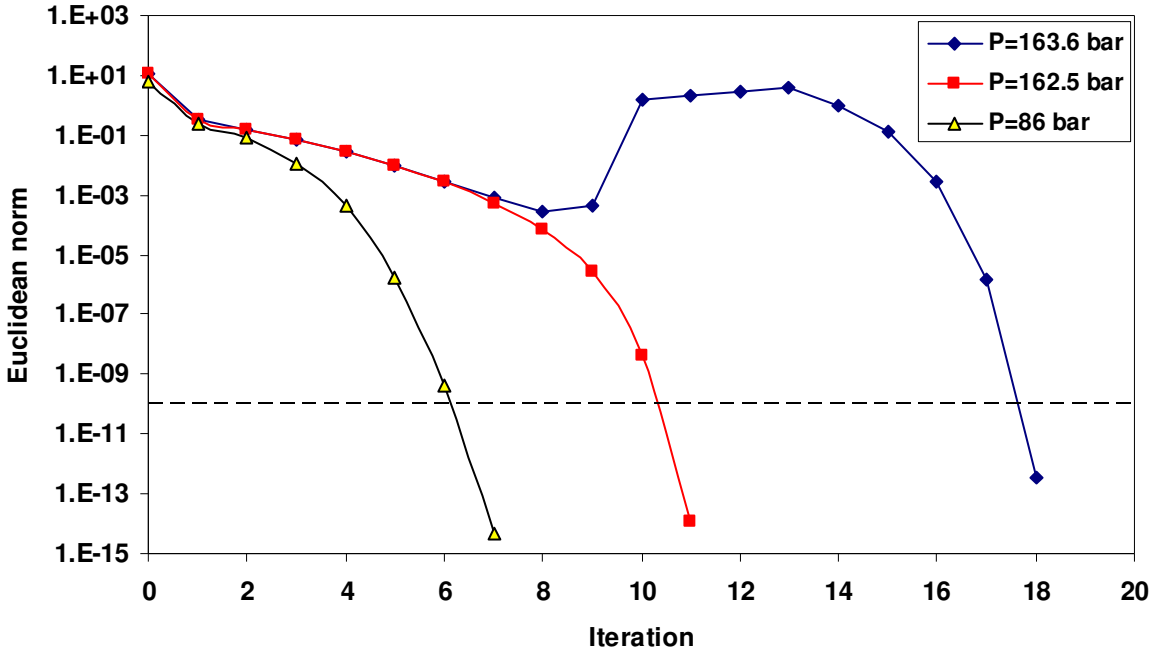

Fig. 4 Euclidean norms during iterations at various pressures; SJ15 Oil at T=383.15 K and r=10 nm (type L initialization)

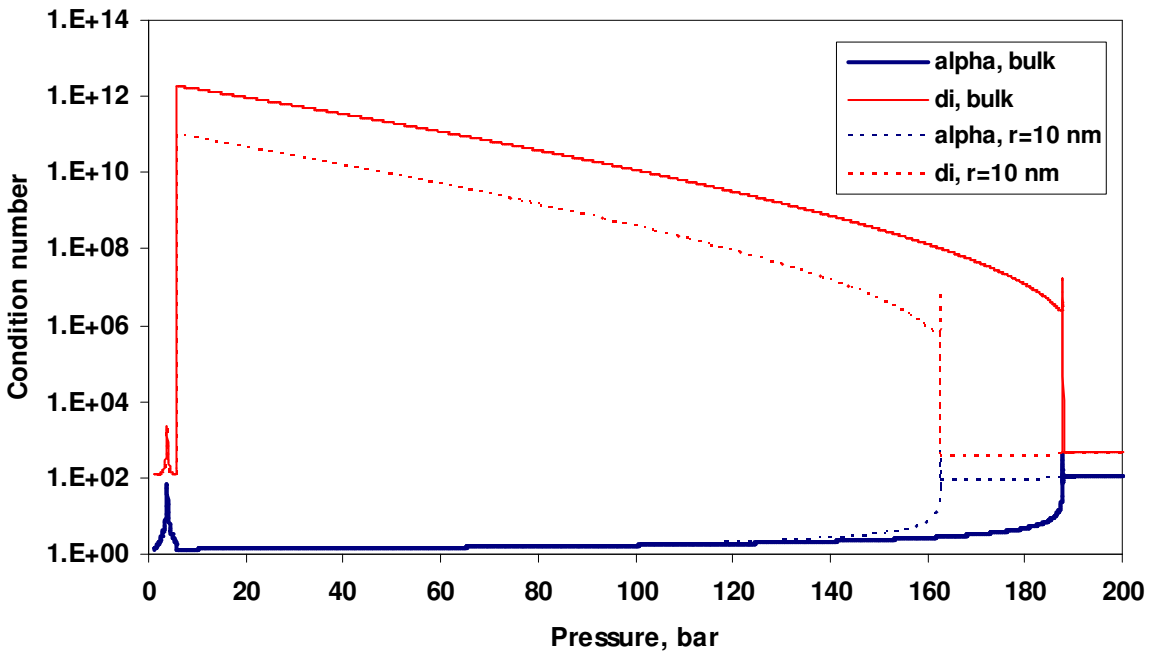

Fig. 5 Condition numbers (at the solution) vs. pressure; SJ15 Oil at T=383.15 K (type L initialization)

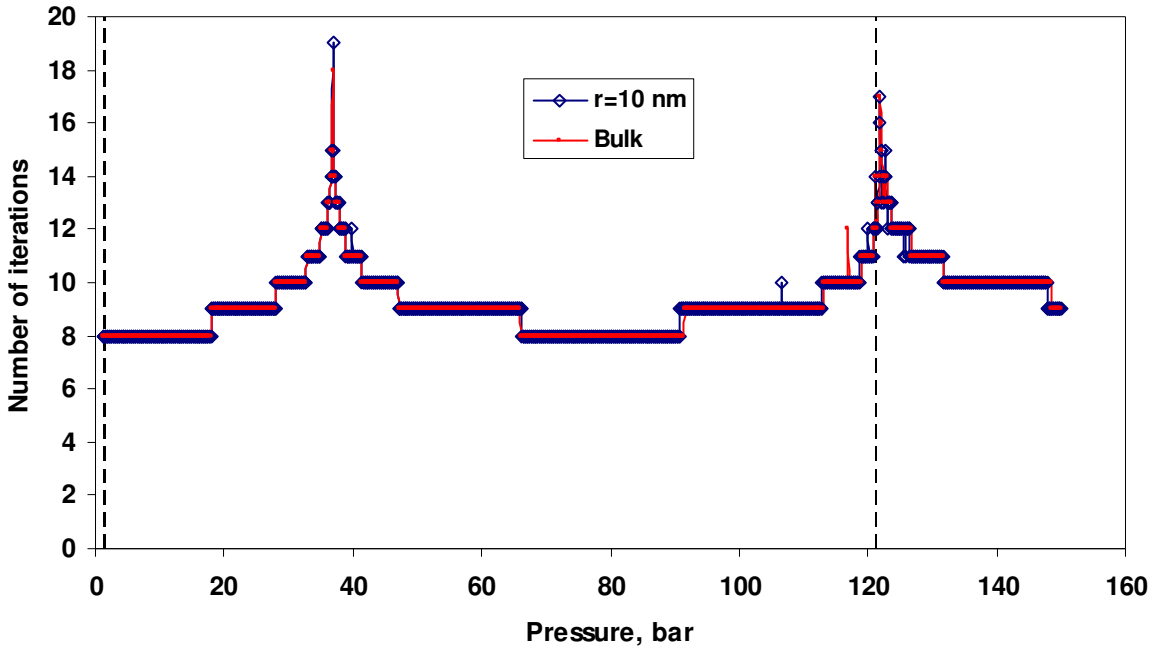

Fig. 6 Number of iterations vs. pressure; SJ15 Oil at T=700 K (type V initialization)

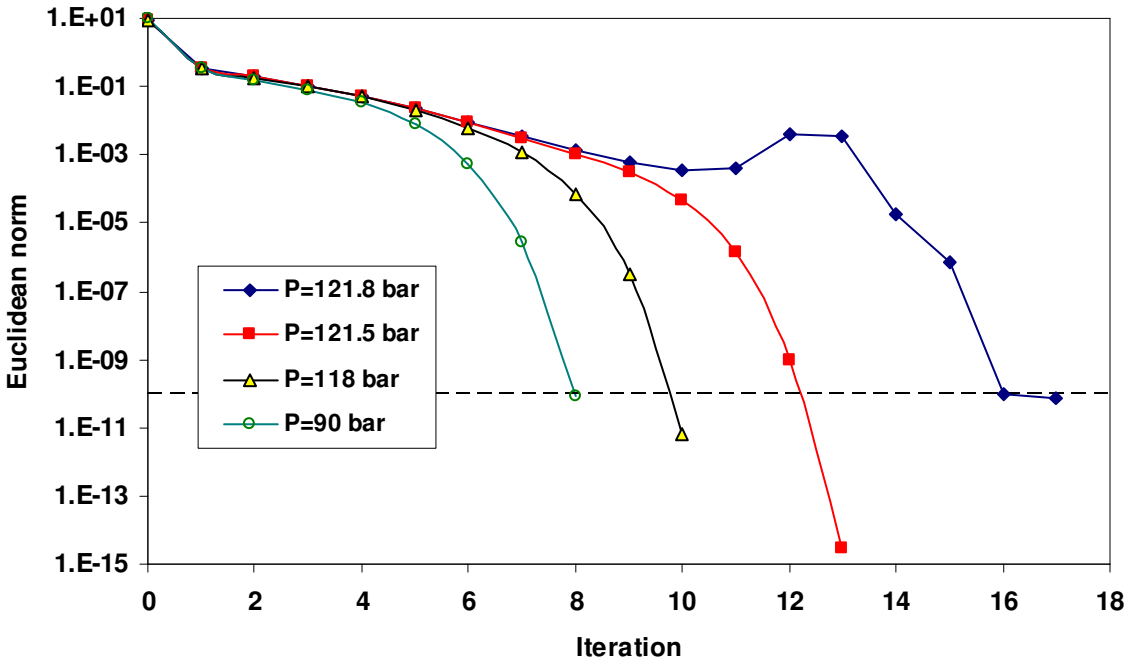

Fig. 7 Euclidean norms during iterations at various pressures; SJ15 Oil at T=700 K and r=10 nm (type L initialization)

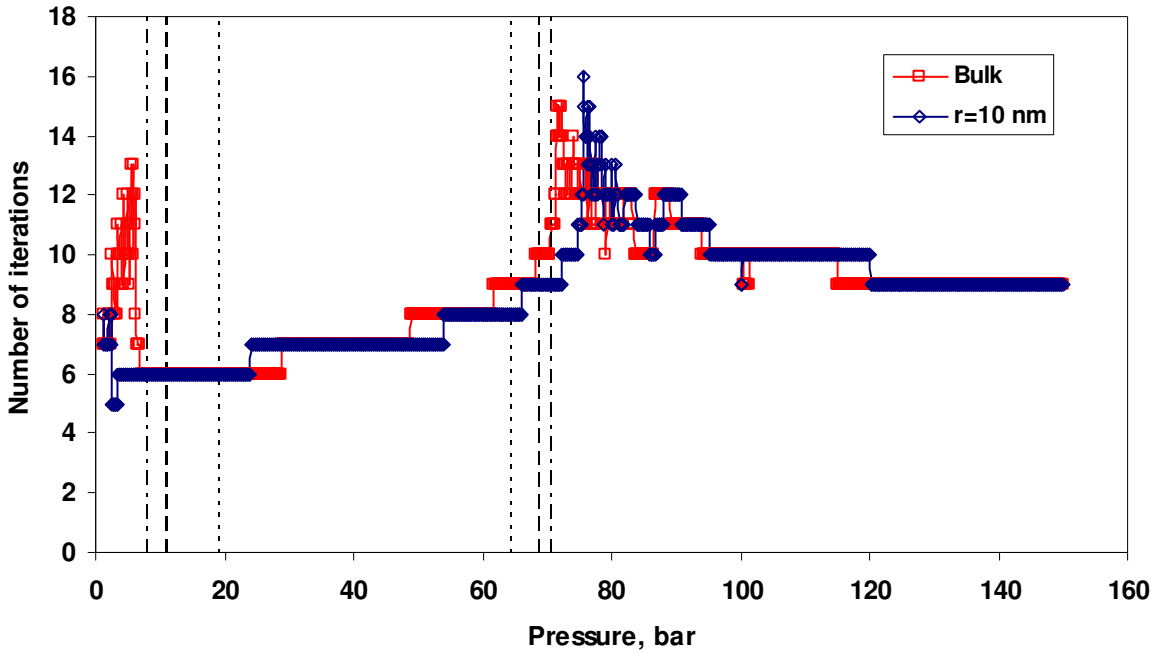

Fig. 8 Number of iterations vs. pressure; SJ15 Oil at T=800 K (type V initialization)

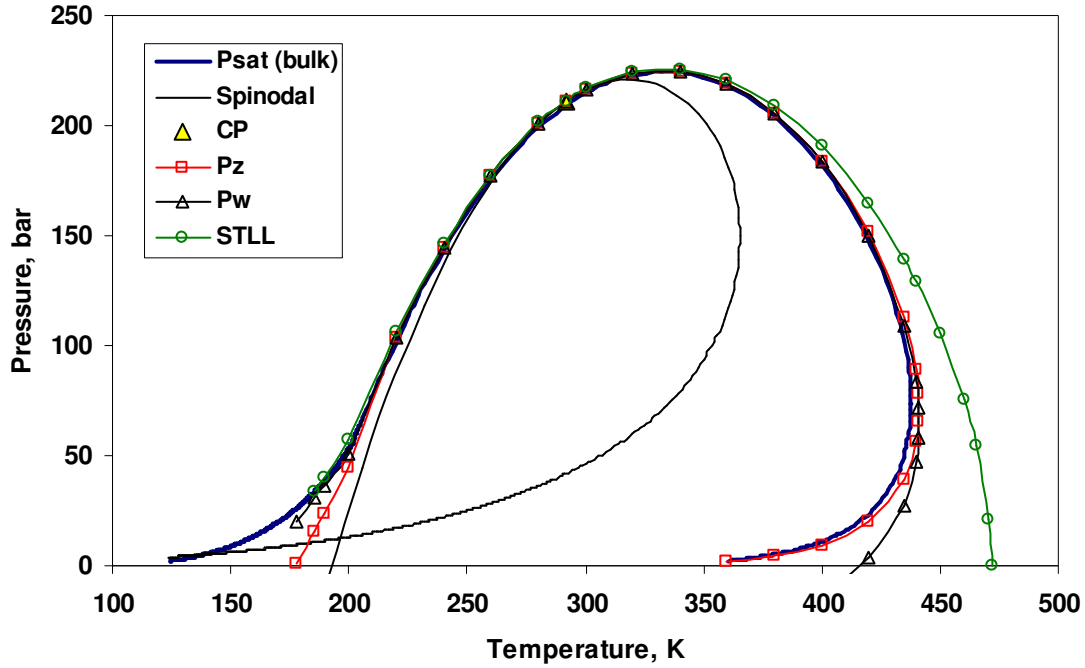

Fig. 9a Phase envelopes of Y8 mixture, r=10 nm

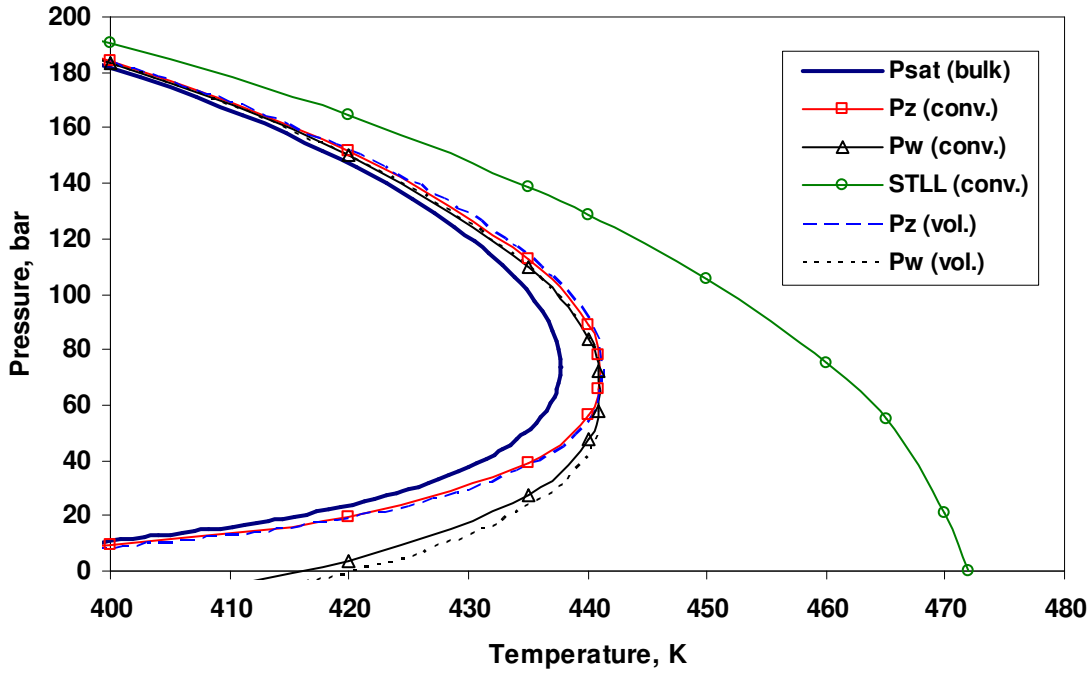

Fig. 9b Phase envelopes of Y8 mixture, r=10 nm (detail)

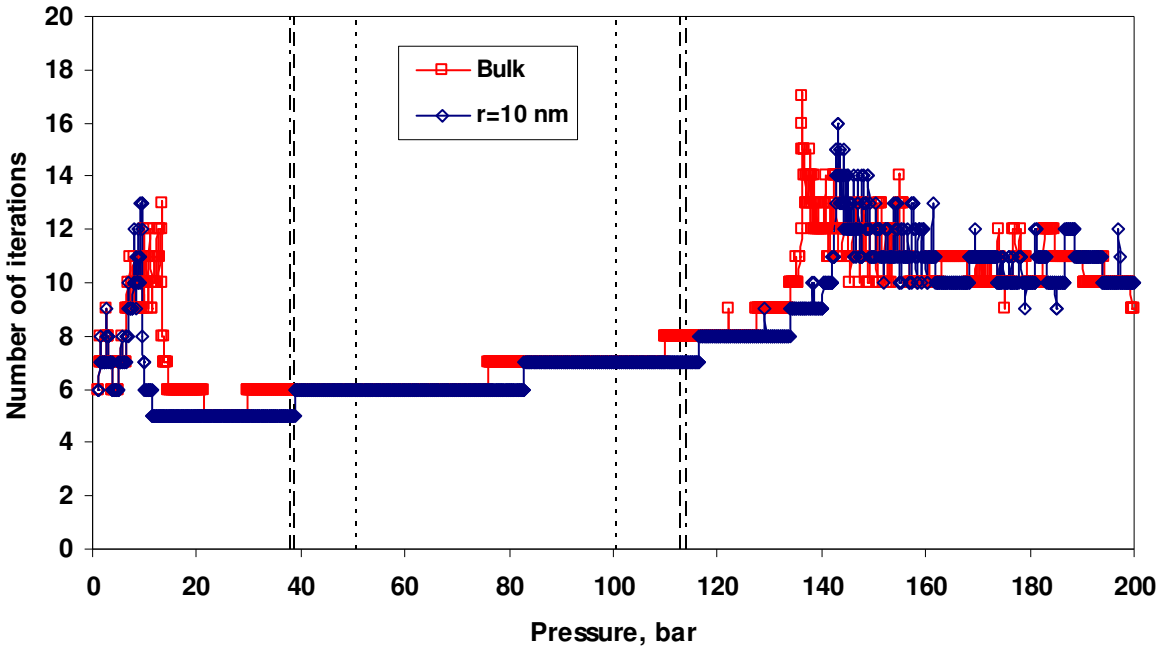

Fig. 10 Number of iterations vs. pressure; Y8 mixture at T=435 K (type V initialization)

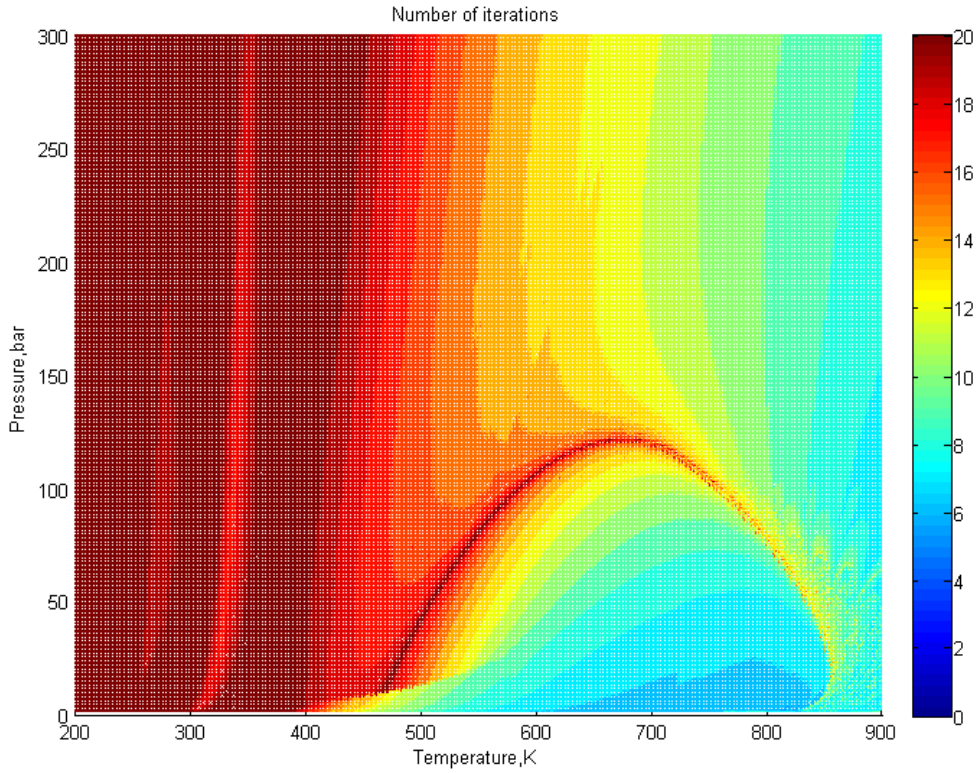

Fig. 11 Number of iterations for the SJ15 oil mixture; type V initialization, r=10 nm

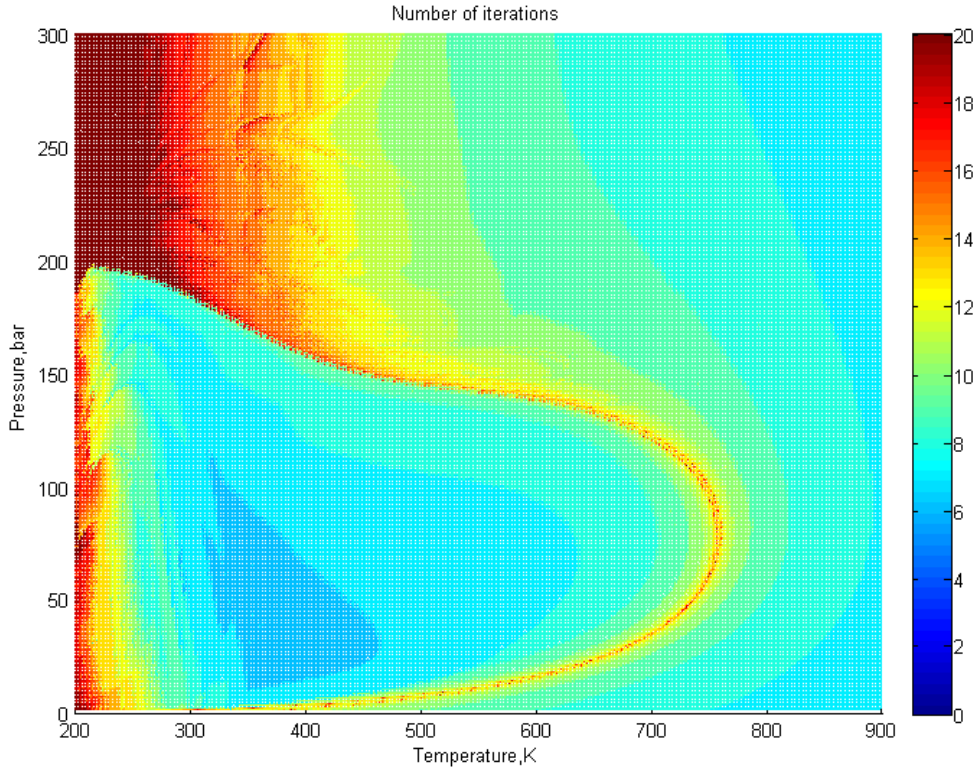

Fig. 12 Number of iterations for the SJ15 oil mixture; type L initialization, r=10 nm

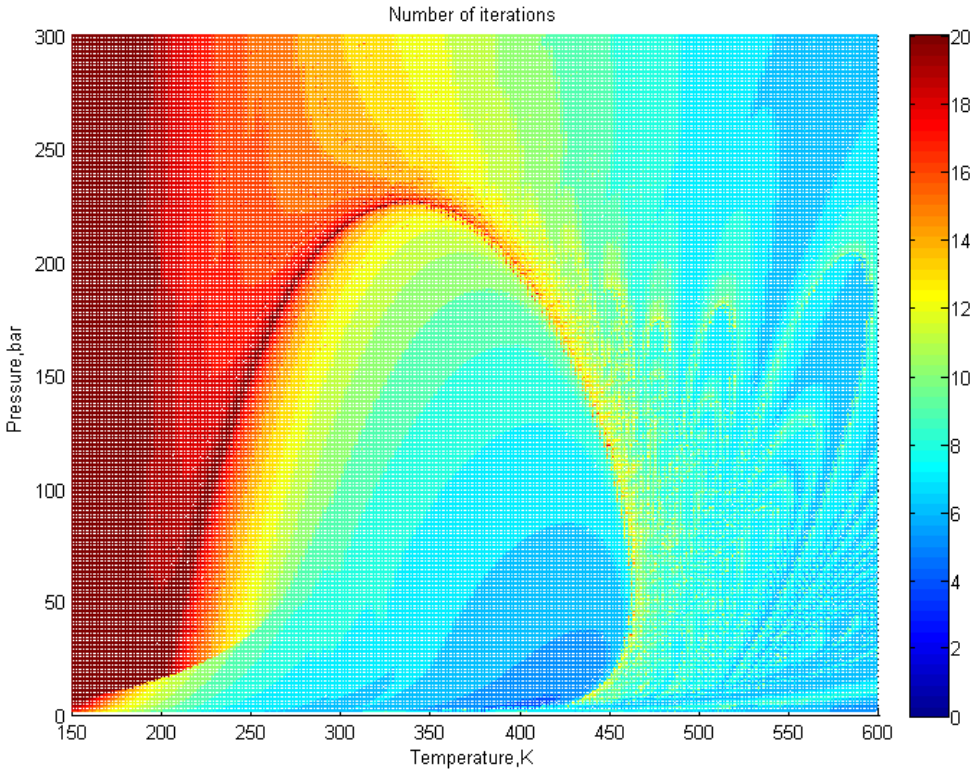

Fig. 13 Number of iterations for the Y8 mixture; type V initialization, r=10 nm

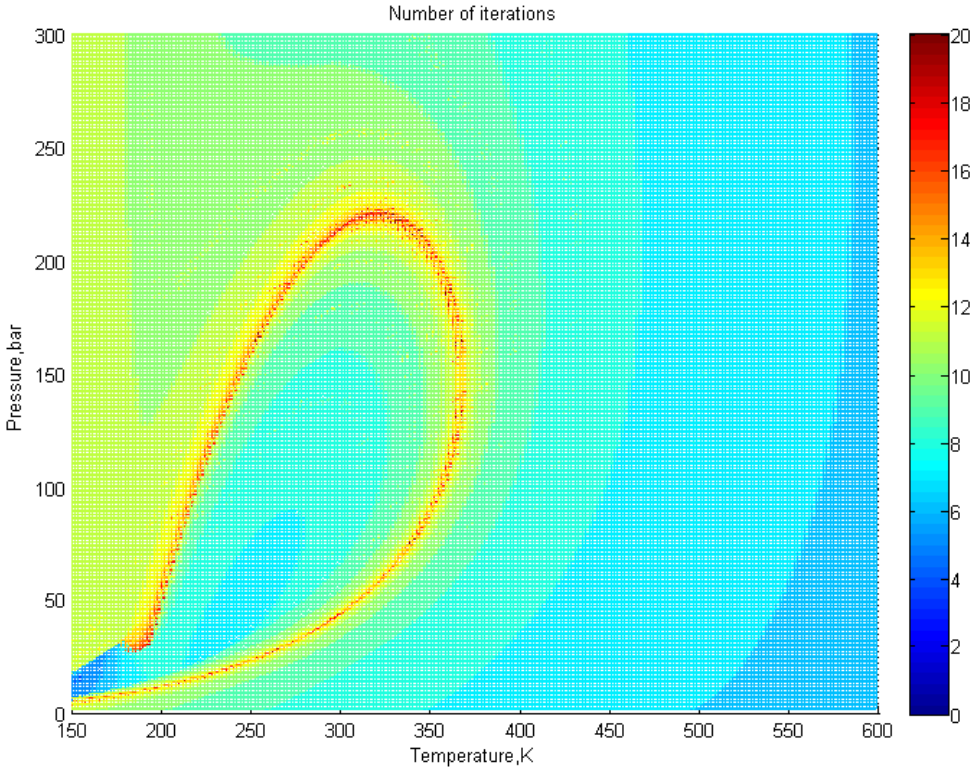

Fig. 14 Number of iterations for the Y8 mixture; type L initialization, r=10 nm

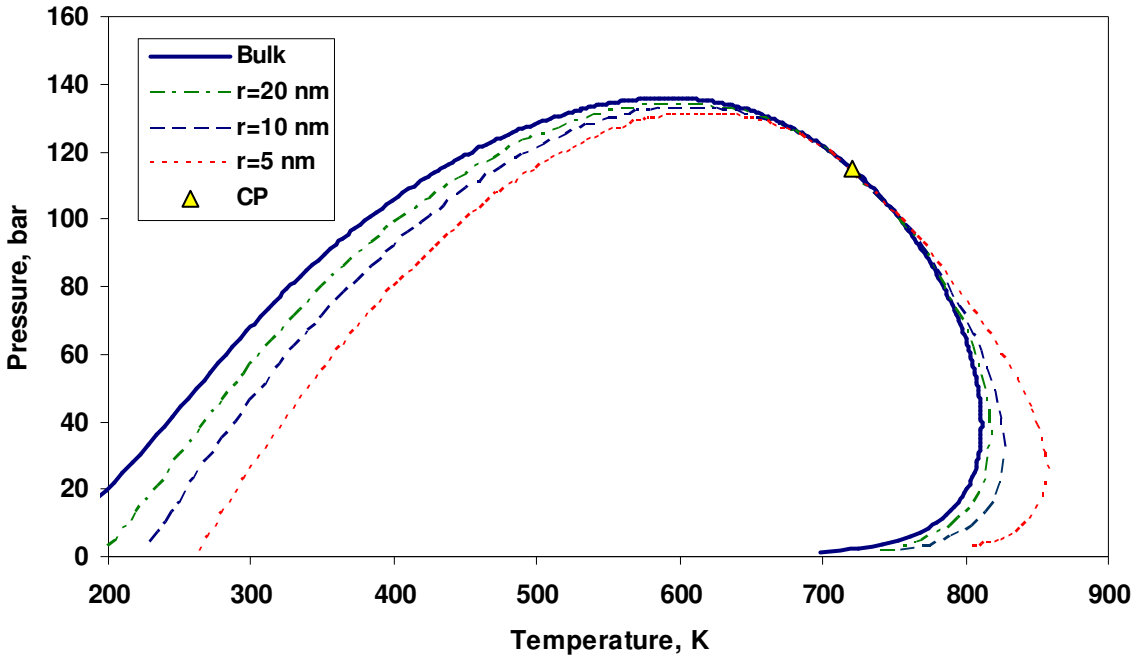

Fig. 15 Influence of capillary radius on phase envelopes of SJ15 Oil

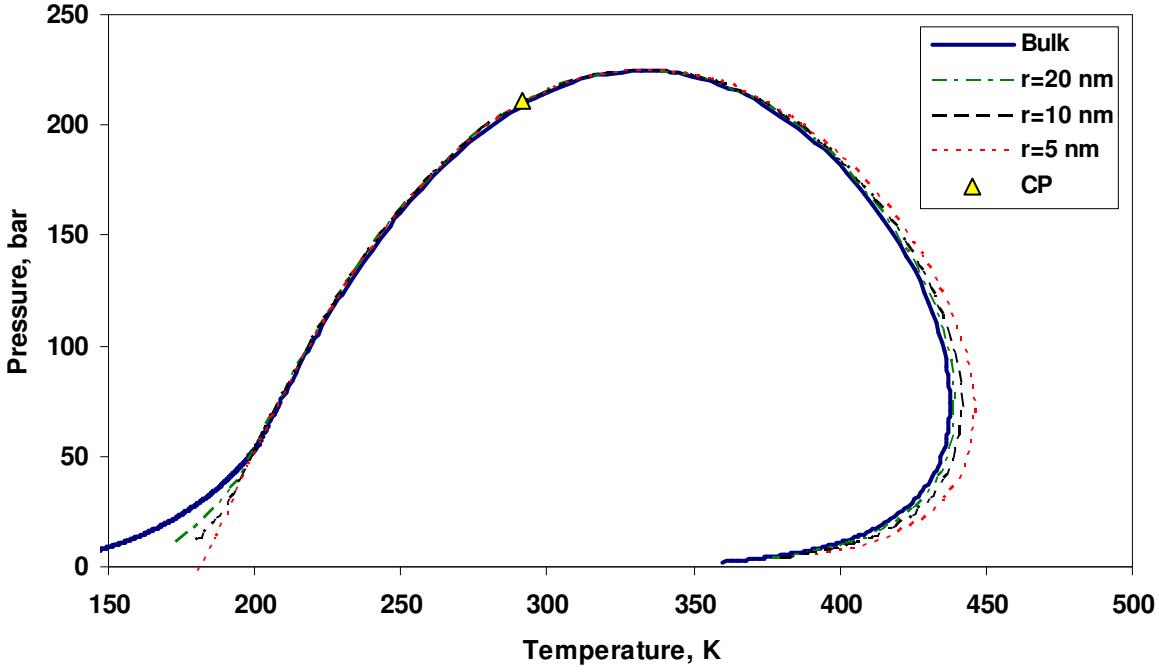

Fig. 16 Influence of capillary radius on phase envelopes of Y8 mixture

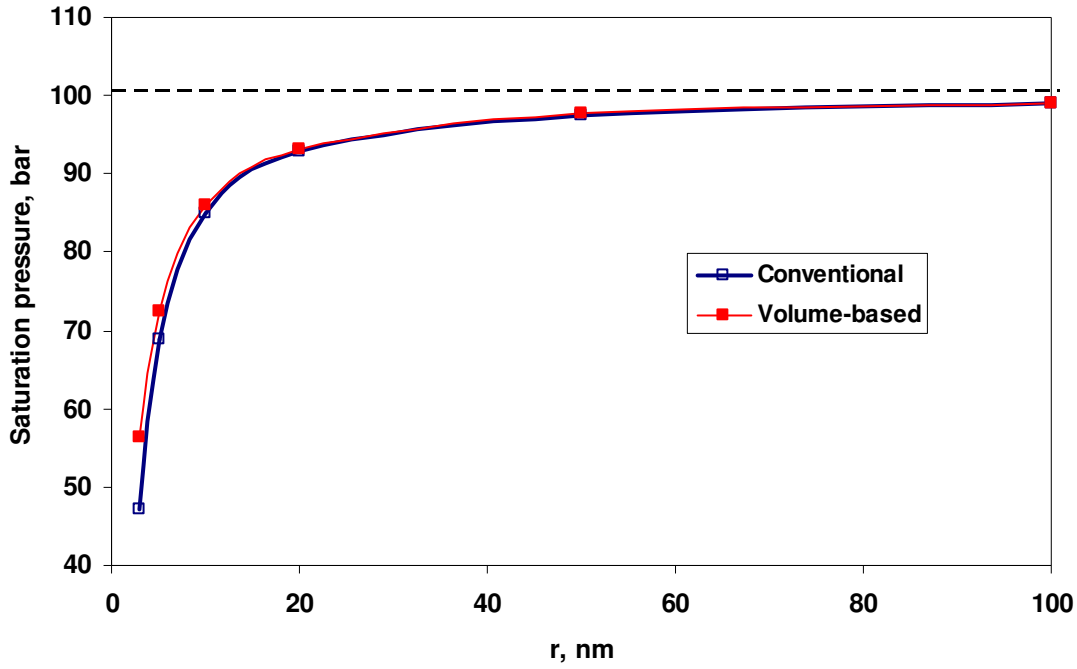

Fig. 17 Influence of capillary radius on saturation pressures; SJ15 Oil at T=383.15 K

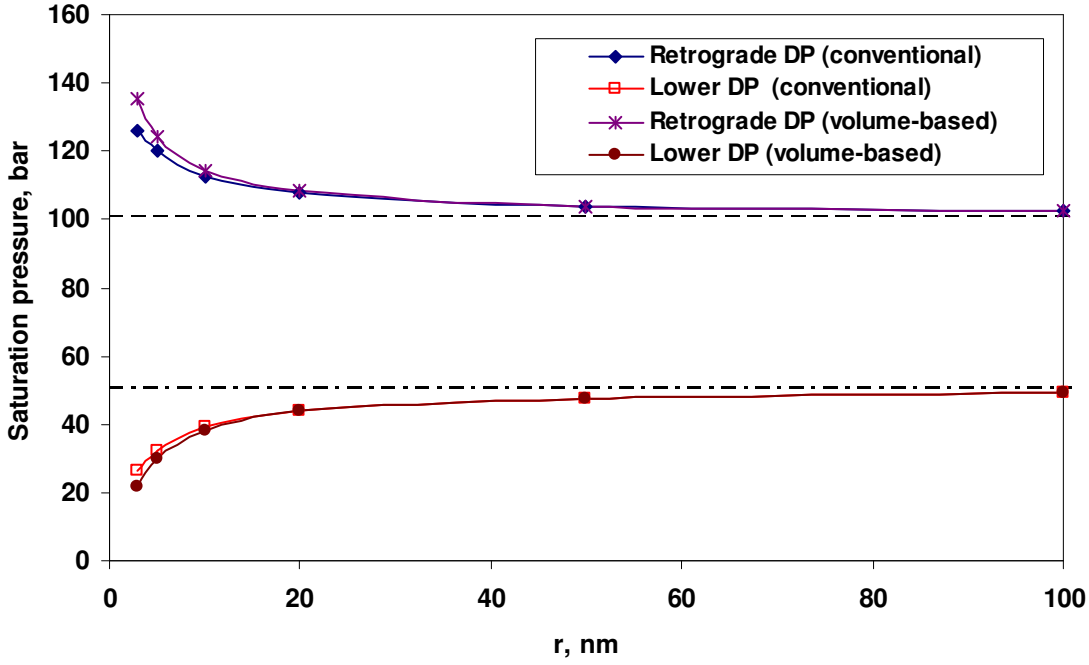

Fig. 18 Influence of capillary radius on saturation pressures; Y8 mixture at T=435 K

Table 1 Composition and component properties of the Y8 mixture

Component	z_i	T_{ci}, K	P_{ci}, bar	ω_i	Π_i
C_1	0.8097	190.56	45.99	0.011	72.60
C_2	0.0566	305.32	48.72	0.099	110.50
C_3	0.0306	369.83	42.48	0.152	150.80
nC_5	0.0457	469.70	33.70	0.252	231.50
nC_7	0.0330	540.20	27.40	0.350	310.80
nC_{10}	0.0244	617.70	21.10	0.490	431.15

Table 2 Average number of iterations for SJ15 and Y8 mixtures, *r*=10 nm

Mixture	Init.	Capillary effects	Bulk fluid
SJ15	L	10.06 [9.42]	9.88 [9.17]
	V	15.09 [12.78]	15.08 [12.76]
Y8	L	8.57 [8.09]	8.54 [8.18]*
	V	11.06 [8.95]	11.08 [8.92]*

* data from Ref. [42]; in brackets results for reduced temperature windows.